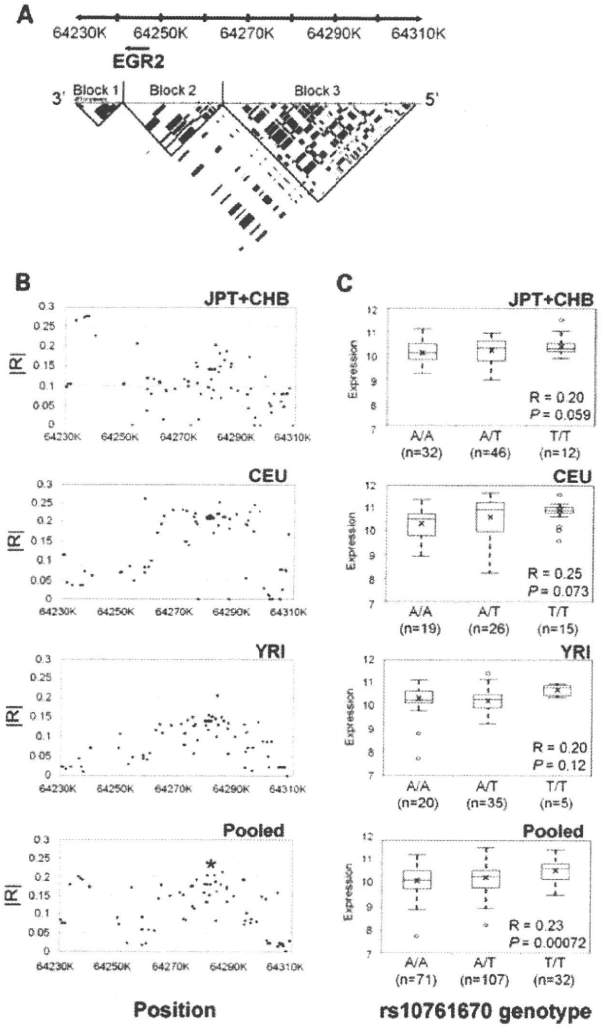


**Figure 1.** The correlation between *EGR2* expression and SNP genotype. (**A**) Three LD blocks were identified in the 80-kb region surrounding the *EGR2* gene using genotype data of HapMap Japanese (JPT) samples. (**B**) The correlation between *EGR2* expression and SNP genotypes (0, 1, 2) using gene expression data from EBV-transformed lymphoblastoid cell lines of HapMap individuals. The analyses of individual populations [JPT + Han Chinese (CHB), European (CEU) and African (YRI)], and of a pool of all of the populations, are shown. |R|: the absolute value of the correlation coefficient between *EGR2* expression and SNP genotype. The asterisk (*) indicates rs10761670. (**C**) Liner regression analysis of the relationship between the rs10761670 genotype and *EGR2* expression (JPT + CHB: $n = 90$; CEU: $n = 60$; YRI: $n = 60$; pooled: $n = 210$). The $x$-axis shows the rs10761670 genotypes (AA, AT, TT) and the $y$-axis represents the $\log_2$-transformed *EGR2* expression level. Top bar of the box-plot represents maximum value and the lower bar represents minimum value. The top of box is third quartile, the bottom of box is first quartile and the middle bar is median value. The x-mark is mean value and the circle is outlier.

association study in the *EGR2* region. Tag SNPs were selected from the HapMap database for association tests. We selected a total of 14 tag SNPs with MAF > 0.10 from the LD blocks described above. Nine of these tag SNPs were from block 3, which spanned the 5′ region of *EGR2* and contained the potential regulatory variants described above, with a threshold value of $r^2 > 0.8$, and the other five SNPs were from blocks 1 and 2 with a threshold value of $r^2 > 0.5$ (Table 1). We initially genotyped 376 SLE cases for the tag SNPs and compared their allele frequencies with those of 940 control individuals. We identified two SNPs (rs10761670 and rs955696) which showed significant association with SLE susceptibility [rs10761670: OR = 1.19 (95% CI 1.00–1.41), $P = 0.049$ and rs955696: OR = 1.23 (95% CI 1.02–1.48), $P = 0.033$, respectively, Table 1]. These SNPs are located in block 3 in the 5′ region of *EGR2*. To validate the case–control association test, we performed a replication study for these two SNPs using additional two sets of SLE cohorts (second set: 293 SLE cases and 881 controls; third set: 223 SLE cases and 658 controls). The association was replicated only for rs10761670 [second set: OR = 1.23 (95% CI 1.02–1.49), $P = 0.029$ and third set: OR = 1.30 (95% CI 1.05–1.62), $P = 0.018$, Table 2], although the possibility remained that the negative results in rs955696 was due to insufficient statistical power of the cohort sets (0.62 and 0.52 for second and third sets, respectively). No heterogeneity was detected among the associations of three cohorts ($P = 0.83$ in a Mantel–Haenszel analysis), and the combined analyses showed a statistically significant association of rs10761670 with SLE susceptibility [OR = 1.23 (95% CI 1.10–1.37), $P = 0.00023$, Table 2]. Both dominant and recessive models showed significant associations in rs10761670 in the pooled set [dominant model: OR = 1.33 (95% CI 1.09–1.62), $P = 0.0045$ and recessive model: OR = 1.32 (95% CI 1.11–1.57), $P = 0.0016$]. After adjustment for gender by a logistic regression analysis, rs10761670 still showed a significant association with SLE susceptibility in the combined set [882 SLE cases and 2467 controls, OR = 1.23 (95% CI 1.09–1.38), $P = 0.00070$].

As previous studies have demonstrated that multiple genes, including *PTPN22*, *STAT4*, *TNFAIP3* and *CD244* (29), increase the risk of both SLE and rheumatoid arthritis (RA), we examined the association of *EGR2* with RA susceptibility using two sets of RA cohorts (first set, 1112 RA cases and 940 controls; second set, 830 RA cases and 881 controls). A significant association was observed in the first set [OR = 1.21 (95% CI 1.07–1.37), $P = 0.0020$], but we did not identify a significant association in the second set [OR = 1.09 (95% CI 0.95–1.24), $P = 0.22$]. The combined analyses showed a statistically significant association with RA susceptibility [OR = 1.15 (95% CI 1.05–1.26), $P = 0.0019$] (Table 3). These results suggested that the *EGR2* polymorphism increased the risk of RA as well as of SLE.

### Search for regulatory SNPs

To identify causal variants, we examined whether nuclear transcription factors bind to genomic sequences surrounding the SNPs and compared the binding ability of susceptible alleles with that of non-susceptible alleles. We selected 15 SNPs that are in complete linkage disequilibrium (LD) with rs10761670 ($r^2 = 1.0$) using the genotype data of Japanese HapMap samples. These SNPs were examined by electrophoretic mobility shift assay (EMSA) using nuclear extracts from an EBV-transformed lymphoblastoid cell line (PSC cells). We found allelic differences in the binding ability of two

**Table 1.** Association analysis of *EGR2* with SLE susceptibility

| dbSNP ID | Allele (1/2) | LD blocks | Number of subjects | | Frequency of allele 1 | | Odds ratio (95%CI)[b] | *P*-value (allele)[a] |
|---|---|---|---|---|---|---|---|---|
| | | | Case | Control | Case | Control | | |
| rs10995312 | C/T | Block 1 | 376 | 940 | 0.54 | 0.51 | 1.12 (0.94–1.33) | 0.20 |
| rs224278 | A/G | Block 2 | 375 | 933 | 0.64 | 0.63 | 1.03 (0.86–1.22) | 0.77 |
| rs224285 | A/C | | 374 | 934 | 0.23 | 0.22 | 1.09 (0.89–1.34) | 0.40 |
| rs224292 | G/A | | 376 | 934 | 0.80 | 0.77 | 1.16 (0.94–1.43) | 0.16 |
| rs11817939 | A/G | | 374 | 934 | 0.89 | 0.87 | 1.18 (0.91–1.53) | 0.22 |
| rs2136613 | A/G | Block 3 | 376 | 934 | 0.36 | 0.35 | 1.01 (0.85–1.21) | 0.88 |
| rs7078554 | A/T | | 374 | 939 | 0.24 | 0.23 | 1.07 (0.87–1.30) | 0.52 |
| rs224307 | G/A | | 375 | 934 | 0.66 | 0.63 | 1.14 (0.95–1.36) | 0.16 |
| rs10761670 | T/A | | 375 | 939 | 0.55 | 0.51 | 1.19 (1.00–1.41) | 0.049 |
| rs10995335 | G/A | | 375 | 940 | 0.90 | 0.88 | 1.16 (0.88–1.53) | 0.30 |
| rs10995337 | C/T | | 374 | 939 | 0.91 | 0.89 | 1.25 (0.93–1.68) | 0.13 |
| rs3939306 | T/C | | 376 | 940 | 0.27 | 0.26 | 1.06 (0.88–1.28) | 0.55 |
| rs949566 | C/G | | 376 | 940 | 0.81 | 0.78 | 1.19 (0.97–1.48) | 0.10 |
| rs955696 | C/T | | 376 | 938 | 0.30 | 0.26 | 1.23 (1.02–1.48) | 0.033 |

[a]*P*-value (allele) was calculated using an allele frequency comparison test.
[b]95% CI = 95% confidence interval.

**Table 2.** Replication study and combined analysis of *EGR2* with SLE susceptibility

| dbSNP ID | Allele (1/2) | Case–control cohorts | Number of subjects | | Frequency of allele 1 | | Odds ratio (95%CI)[b] | *P*-value (allele)[a] |
|---|---|---|---|---|---|---|---|---|
| | | | Case | Control | Case | Control | | |
| rs10761670 | T/A | 2nd | 287 | 876 | 0.56 | 0.51 | 1.23 (1.02–1.49) | 0.029 |
| | | 3rd | 220 | 652 | 0.57 | 0.51 | 1.30 (1.05–1.62) | 0.018 |
| | | Combined analysis[c] | 882 | 2467 | 0.56 | 0.51 | 1.23 (1.10–1.37) | 0.00023 |
| rs955696 | C/T | 2nd | 290 | 873 | 0.28 | 0.26 | 1.12 (0.91–1.38) | 0.30 |
| | | 3rd | 223 | 654 | 0.31 | 0.27 | 1.24 (0.98–1.57) | 0.073 |
| | | Combined analysis[c] | 889 | 2465 | 0.30 | 0.26 | 1.19 (1.06–1.34) | 0.0040 |

[a]*P*-value (allele) was calculated using an allele frequency comparison test.
[b]95% CI = 95% confidence interval.
[c]The Mantel–Haenszel method was used for the combined analysis of first, second and third sets.

**Table 3.** Association analysis of *EGR2* with RA susceptibility

| dbSNP ID | Allele (1/2) | Case–control cohorts | Number of subjects | | Frequency of allele 1 | | Odds ratio (95%CI)[b] | *P*-value (allele)[a] |
|---|---|---|---|---|---|---|---|---|
| | | | Case | Control | Case | Control | | |
| rs10761670 | T/A | 1st | 1105 | 939 | 0.56 | 0.51 | 1.21 (1.07–1.37) | 0.0020 |
| | | 2nd | 827 | 877 | 0.53 | 0.51 | 1.09 (0.95–1.24) | 0.22 |
| | | Combined analysis[c] | 1932 | 1816 | 0.55 | 0.51 | 1.15 (1.05–1.26) | 0.0019 |

[a]*P*-value (allele) was calculated using an allele frequency comparison test.
[b]95% CI = 95% confidence interval.
[c]The Mantel–Haenszel method was used for the combined analysis of first and second sets.

SNPs, rs1412554 and rs1509957. For rs1412554, the intensity of the shifted band was higher for the susceptible allele than for the non-susceptible allele. In contrast, a particular band was seen specifically to the non-susceptible allele for rs1509957 (Fig. 2A). Competition assays with unlabeled oligonucleotides showed that these complexes were specific for each oligonucleotide. Similar results were obtained when nuclear extracts of Jurkat cells were tested (Fig. 2A).

The transcriptional activity of rs1412554 and rs1509957 was then analyzed using luciferase assays. Allele specific constructs containing the SNPs and surrounding genomic sequences were constructed and transfected into Jurkat cells. Cells transfected with the susceptible allele of rs1412554 displayed a 1.2-fold greater enhancement of transcriptional activity than cells transfected with the non-susceptible allele (Fig. 2B). In contrast, only cells transfected with the

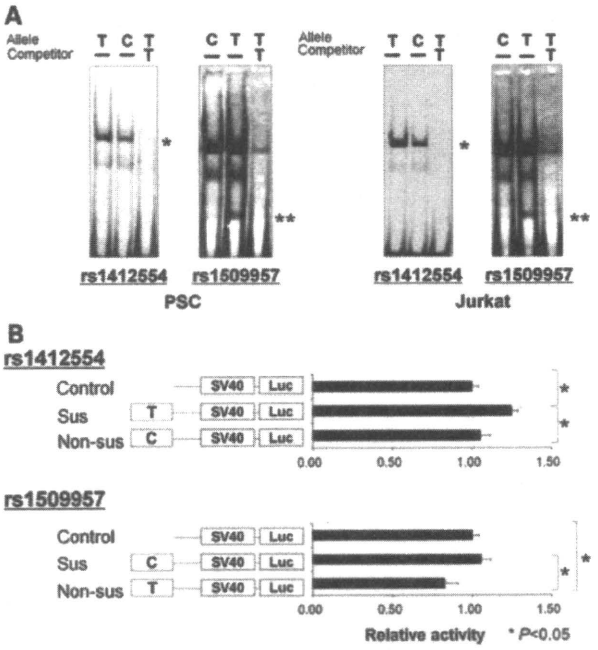


**Figure 2.** Transcriptional activity is affected by rs1412554 and rs1509957. (**A**) EMSAs were performed with nuclear extracts from PSC and Jurkat cells. Biotin-labeled 25-bp oligonucleotides corresponding to each SNP (rs1412554 and rs1509957) served as probes for the susceptible (Sus), and the non-susceptible (Non-sus), allele, respectively, and the abilities of nuclear factors to bind to these oligonucleotides were evaluated (for rs1412554: Sus = T, Non-sus = C; for rs1509957: Sus = C, Non-sus = T). Unlabeled oligonucleotides were used for competition assays. A single asterisk (*) and double asterisks (**) indicate bands showing allelic differences in rs1412554 and rs1509957, respectively. PSC cells (Left) and Jurkat cells (Right). (**B**) Transcriptional activities of the 31-bp genomic sequences around SNPs [rs1412554 (T/C) and rs1509957 (C/T)] were evaluated by luciferase assays. Each 31-bp oligonucleotide corresponding to these genomic sequences was inserted into the pGL3-promoter vector upstream of the SV 40 promoter and allele-specific constructs were transfected into Jurkat cells. Relative promoter activity was expressed as the ratio of the luciferase activity of each allele specific construct to the luciferase activity of the pGL3-promoter control vector. Data are presented as the mean ± SEM. Each experiment was independently repeated three times and each sample was studied in sextuplicate. *$P < 0.05$ by Student's *t*-test. Rs1412554 (top) and rs1509957 (bottom).

non-susceptible allele of rs1509957 displayed a repression of transcriptional activity (Fig. 2B). Therefore, rs1412554 and rs1509957 may contribute to transcriptional modulation of the *EGR2* gene, suggesting that these two SNPs could be candidates of causal variants in this chromosomal region.

## DISCUSSION

In the present study, we demonstrated that polymorphisms in the *EGR2* gene are associated with SLE susceptibility, presumably through up-regulating the gene expression. An SNP in the 5′ flanking region of *EGR2*, termed rs10761670, showed the highest correlation between *EGR2* expression and its genotype. Furthermore, in case–control association tests, the peak association with SLE susceptibility was observed for rs10761670. This correspondence between the two independent associations (gene expression and disease susceptibility) strongly indicates the presence of disease-causing regulatory variants in this region. Two SNPs, rs1412554 and rs1509957, which are in complete LD with rs10761670, and were shown to affect the binding of transcription factors and to modulate gene expression in *in vitro* assays, are candidate SNPs for the causal variants, although other undiscovered variants may also contribute to the regulation of gene expression.

When the effective size of the *EGR2* polymorphism that contributes to disease risk is measured as OR, this size is relatively small compared with that of other loci described in recent GWASs of SLE, suggesting that *EGR2* polymorphism has a moderate risk for an individual. However, the risk allele of rs10761670 is common in the population (the allele frequency = 0.51). This indicates that the *EGR2* polymorphism contributes to the onset of SLE in a wide population in contrast to rare but high penetrant variants. We calculated the population attributable risk proportion (PARP) to assess the reduction in susceptibility to SLE, if these risk alleles were removed from the population, and the PARP for rs10761670 in *EGR2* was 0.088.

In GWASs of CD in Caucasian populations, two landmark SNPs (rs224136 and rs10761659) were located in the intergenic region between *ZNF365* and *EGR2* (at the 3′ side of *EGR2*). Because T cells are considered to play a significant role in the pathogenesis of CD, *EGR2*, which is a potential regulator of TCR signaling, is a strong candidate for CD susceptibility at this locus. Therefore, genetic variations with disease-causing potential in this region could potentially be shared genetic risk factors for CD and SLE. However, the landmark SNP identified in the present study (rs10761670) is located in the 5′ flanking region of *EGR2* and is not in strong LD ($r^2 < 0.20$) with SNPs of CD (rs224136 and rs10761659) in either Japanese or Caucasian populations. This finding implies that causal variants may be different between SLE and CD or may differ between ethnic populations. Therefore, comparative analyses of both diseases between populations are needed to clarify this problem.

In mice, *Egr2* conditional knockout in $CD2^+$ T cells results in the development of a lupus-like autoimmune disease, where complete loss of *Egr2* function may lead to the loss of regulation of effector T cells and self-reactive T cells (20). In addition, transduction of *Egr2* into naïve $CD4^+$ T cells differentiates them to IL-10-secreting $CD4^+CD25^-LAG3^+$ regulatory T cells that would suppress self-reactive cells (21). These protective roles of *Egr2* against autoimmunity in mice contradict our findings that enhanced expression of *EGR2* may increase SLE susceptibility in humans. Similar observations were reported for the *PTPN22* gene, another established susceptibility gene for both SLE and RA (4,30). *PTPN22* encodes a tyrosine phosphatase, LYP that has an inhibitory effect on TCR signaling. For LYP, a non-synonymous SNP (rs2276601, R620W) was associated with disease susceptibility, and increased inhibition of TCR signaling was shown with the disease risk allele W620 (31). Furthermore, knockout of *Pep*, the murine ortholog of *PTPN22*, leads to various immune abnormalities, including expansion of effector T cells and increased antibody production (32). Taken together, enhanced negative regulation of T cells by inhibitory components such as *EGR2* and *PTPN22* may lead to tolerance

breakdown in human diseases, while complete loss of function of these components may result in a hyperactive or autoimmune response in mice. Moreover, another plausible explanation for the role of *EGR2* in human autoimmunity has been recently raised by an analysis on *Egr2* deficient thymocytes in mice, which concluded that *Egr2* plays a central role in the up-regulation of the survival molecule *Bcl-2* during the positive selection of thymocytes (33). As overexpression of *Bcl-2* has been shown to result in the increased self-reactive thymocytes (34), up-regulated expression of *Egr2* may also lead to increased selection of self-reactive thymocytes.

In conclusion, *EGR2* is a genetic risk factor for SLE as well as for RA, for which increased gene expression may contribute to disease pathogenesis. Analyses of *EGR2* in other autoimmune disorders, including CD, are needed to elucidate its precise role in autoimmunity.

## MATERIALS AND METHODS

### Subjects

Three independent sets of SLE ($n = 376$, 293 and 223) and two independent sets of RA ($n = 1112$ and 830) patients, and of control subjects ($n = 940$, 881 and 658), were enrolled in the study through medical institutes in Japan. The control subjects in the first set were the members of Midousuji Rotary Club and those in third set was recruited through Pharma SNP Consortium (35). All subjects were self-identified Japanese. SLE subjects met the revised American College of Rheumatology (ACR) criteria for SLE (1) and RA subjects met the revised ACR criteria for RA (36). All control subjects were confirmed to be not affected with autoimmune diseases including SLE and RA by reviewing their medical records. All subjects provided informed consent to their participation in the study, as approved by the Ethics Committee of the Center for Genomic Medicine, RIKEN. DNA was extracted from peripheral blood cells using a standard protocol.

### SNP discovery

Unknown SNPs were revealed by direct sequencing of the DNA of 96 individuals affected with SLE. DNA fragments were amplified for sequencing with the appropriate primers and were purified using a MultiScreen PCR filter plate (Millipore, Billerica, MA, USA). The amplified DNAs were sequenced using the BigDye Terminator v3.1 Cycle Sequencing kit (Applied Biosystems, Foster City, CA, USA) and signals were detected using an Applied Biosystems ABI 3700 DNA Analyzer.

### Genotyping

We selected 14 tag SNPs from an 80-kb region on 10q21.3, which comprised three LD blocks and included the *EGR2* gene, using the HapMap data of the Japanese population and Haploview software, v.4.0. These SNPs were genotyped using TaqMan SNP genotyping assays (Applied Biosystems) as indicated by the manufacturer. Fluorescence was detected using an ABI Prism 7900HT Sequence Detection System (Applied Biosystems). All SNPs were successfully genotyped with call rates >0.99 and were in Hardy–Weinberg equilibrium in control subjects ($P > 0.01$).

### Electrophoretic mobility shift assays

PSC (an EBV-transformed lymphoblastoid cell line) and Jurkat cells were grown in RPMI 1640 medium supplemented with 10% fetal bovine serum and antibiotics. Nuclear extracts were prepared as previously described (37). In brief, following stimulation with 50 ng/ml phorbol myristate acetate (Sigma, St Louis, MO, USA) for 2 h, centrifuged cells were collected and resuspended in Buffer A (20 mM HEPES pH 7.6, 20% glycerol, 10 mM NaCl, 1.5 mM $MgCl_2$, 0.2 mM EDTA pH 8.0, 1 mM DTT, 0.1% NP-40 and Protease inhibitor cocktail). The cells were then incubated on ice for 10 min, centrifuged and the pellets were resuspended in Buffer B (20 mM HEPES pH 7.6, 20% glycerol, 500 mM NaCl, 1.5 mM $MgCl_2$, 0.2 mM EDTA pH 8.0, 1 mM DTT, 0.1% NP-40 and Protease inhibitor cocktail). Following incubation on ice for 30 min and then centrifugation to remove cellular debris, the supernatant fraction containing nuclear proteins was collected. Oligonucleotides (25 bp) were designed that corresponded to genomic sequences surrounding the SNPs. Single-stranded 25-bp oligonucleotide probes were labeled using a Biotin 3′ End DNA Labeling Kit (Pierce Biotechnology, Rockford, IL, USA) and sense and antisense oligonucleotides were then annealed. The LightShift Chemiluminescent EMSA kit (Pierce Biotechnology) was used for the detection of DNA–protein interactions. Biotin-labeled probes were incubated with nuclear extracts in a binding reaction mixture (10× binding buffer, 50 ng/μl poly dI-dC, 50% glycerol, 5 mM $MgCl_2$ and 0.05% NP-40) for 20 min at 25°C. In competition studies, unlabeled oligonucleotides (100-fold excess) were preincubated with the nuclear extract and binding reaction mixture for 5 min before addition of the biotin-labeled probes. The DNA–protein complexes were separated on a non-denaturing 5% polyacrylamide gel in 1× TBE (Tris-borate-EDTA) running buffer for 70 min at 150 V. Gel protein–DNA complexes were transferred to a nitrocellulose membrane for 30 min at 380 mA and the transferred complexes were cross-linked to the membrane by exposure to UV light of 120 mJ/cm$^2$ for 1 min. DNA–protein complexes on the membrane were detected using the Chemiluminescent Nucleic Acid Detection Module (Pierce) and a LAS-3000 mini lumino-image analyzer (Fujifilm, Tokyo, Japan). Allelic differences were analyzed using MultiGauge software (Fujifilm) by measuring the intensity of the bands.

### Luciferase assay

Oligonucleotides (31 bp) were designed that corresponded to genomic sequences that included susceptible or non-susceptible alleles. Complementary sense and antisense oligonucleotides were then annealed. To construct luciferase reporter plasmids, the pGL3-Promoter vector (Promega, Madison, WI, USA) was digested with *Mul*I and *Bgl*II and a single copy of a 31-bp oligonucleotide was ligated into the vector upstream of the SV 40 promoter using the TaKaRa Ligation kit ver. 2.1 (TaKaRa, Shiga, Japan). After confirmation of the sequence, these plasmids were purified using

a HiSpeed Plasmid Midi kit (Qiagen, Valencia, CA, USA). Jurkat cells ($5 \times 10^5$), grown as described above, were transfected with 2.5 μg of the constructs and 0.5 μg of the pRL-TK vector (an internal control for transfection efficiency) using the Lipofectamin2000 transfection reagent (Invitrogen, Carlsbad, CA, USA). After 24 h, the cells were collected and luciferase activity was measured using a Dual-Luciferase Reporter Assay system (Promega) and an Ultra Sensitive Tube Luminometer, Lumat LB 9507 (Berthold Technologies, Bad Wildbad, Germany). Each experiment was independently repeated three times and sextuplicate samples were assayed each time.

### Statistical analysis

We used $\chi^2$ contingency table tests to evaluate the significance of differences in allele frequency in the case–control subjects. We defined haplotype blocks using the Solid spine of LD definition of the Haploview v4.0. We performed a Mantel–Haenszel analysis to calculate the pooled *P*-value and odds ratio of two independent association studies. We calculated the power of each cohort for testing association by Quanto Software (http://hydra.usc.edu/gxe/). To adjust for the confounding effects such as gender, we performed a logistic regression analysis using the STATISTICA software (StatSoft). We calculated PARP using the following formula; $\mathrm{PARP} = f(\mathrm{OR}-1)/(1+f(\mathrm{OR}-1)) \times 100$, where $f$ is the allele frequency in the control subjects and OR is the odds ratio. PARP is defined as the reduction of disease incidence that would be achieved if the population had been entirely unexposed. Luciferase assay data were analyzed by Student's *t*-test.

## ACKNOWLEDGEMENTS

We thank K. Kobayashi, K. Shimada, M. Kitazato and all other members of the Laboratory for Autoimmune Diseases, CGM, RIKEN for their advice and technical assistance. We also thank Dr A. Miyatake, the members of the Rotary Club of Osaka-Midosuji District 2660 Rotary International in Japan, and the staffs of the BioBank Japan Project for clinical sample collection.

*Conflicts of Interest statement*. None declared.

## FUNDING

This work was supported by grants from the CGM, RIKEN; the Ministry of Education, Culture, Sports, Science and Technology of Japan (Leading Project); and the Ministry of Health, Labor and Welfare of Japan (Research on Intractable Diseases).

## REFERENCES

1. Hochberg, M.C. (1997) Updating the American College of Rheumatology revised criteria for the classification of systemic lupus erythematosus. *Arthritis Rheum.*, **40**, 1725.
2. Kyogoku, C., Dijstelbloem, H.M., Tsuchiya, N., Hatta, Y., Kato, H., Yamaguchi, A., Fukazawa, T., Jansen, M.D., Hashimoto, H., van de Winkel, J.G. *et al.* (2002) Fcgamma receptor gene polymorphisms in Japanese patients with systemic lupus erythematosus: contribution of FCGR2B to genetic susceptibility. *Arthritis Rheum.*, **46**, 1242–1254.
3. Edberg, J.C., Langefeld, C.D., Wu, J., Moser, K.L., Kaufman, K.M., Kelly, J., Bansal, V., Brown, W.M., Salmon, J.E., Rich, S.S. *et al.* (2002) Genetic linkage and association of Fcgamma receptor IIIA (CD16A) on chromosome 1q23 with human systemic lupus erythematosus. *Arthritis Rheum.*, **46**, 2132–2140.
4. Kyogoku, C., Langefeld, C.D., Ortmann, W.A., Lee, A., Selby, S., Carlton, V.E., Chang, M., Ramos, P., Baechler, E.C., Batliwalla, F.M. *et al.* (2004) Genetic association of the R620W polymorphism of protein tyrosine phosphatase PTPN22 with human SLE. *Am. J. Hum. Genet.*, **75**, 504–507.
5. Sigurdsson, S., Nordmark, G., Goring, H.H., Lindroos, K., Wiman, A.C., Sturfelt, G., Jonsen, A., Rantapaa-Dahlqvist, S., Moller, B., Kere, J. *et al.* (2005) Polymorphisms in the tyrosine kinase 2 and interferon regulatory factor 5 genes are associated with systemic lupus erythematosus. *Am. J. Hum. Genet.*, **76**, 528–537.
6. Fernando, M.M., Stevens, C.R., Sabeti, P.C., Walsh, E.C., McWhinnie, A.J., Shah, A., Green, T., Rioux, J.D. and Vyse, T.J. (2007) Identification of two independent risk factors for lupus within the MHC in United Kingdom families. *PLoS Genet.*, **3**, e192.
7. Remmers, E.F., Plenge, R.M., Lee, A.T., Graham, R.R., Hom, G., Behrens, T.W., de Bakker, P.I., Le, J.M., Lee, H.S., Batliwalla, F. *et al.* (2007) STAT4 and the risk of rheumatoid arthritis and systemic lupus erythematosus. *N. Engl. J. Med.*, **357**, 977–986.
8. Graham, R.R., Cotsapas, C., Davies, L., Hackett, R., Lessard, C.J., Leon, J.M., Burtt, N.P., Guiducci, C., Parkin, M., Gates, C. *et al.* (2008) Genetic variants near TNFAIP3 on 6q23 are associated with systemic lupus erythematosus. *Nat. Genet.*, **40**, 1059–1061.
9. Kozyrev, S.V., Abelson, A.K., Wojcik, J., Zaghlool, A., Linga Reddy, M.V., Sanchez, E., Gunnarsson, I., Svenungsson, E., Sturfelt, G., Jonsen, A. *et al.* (2008) Functional variants in the B-cell gene BANK1 are associated with systemic lupus erythematosus. *Nat. Genet.*, **40**, 211–216.
10. Harley, J.B., Alarcon-Riquelme, M.E., Criswell, L.A., Jacob, C.O., Kimberly, R.P., Moser, K.L., Tsao, B.P., Vyse, T.J., Langefeld, C.D., Nath, S.K. *et al.* (2008) Genome-wide association scan in women with systemic lupus erythematosus identifies susceptibility variants in ITGAM, PXK, KIAA1542 and other loci. *Nat. Genet.*, **40**, 204–210.
11. Hom, G., Graham, R.R., Modrek, B., Taylor, K.E., Ortmann, W., Garnier, S., Lee, A.T., Chung, S.A., Ferreira, R.C., Pant, P.V. *et al.* (2008) Association of systemic lupus erythematosus with C8orf13-BLK and ITGAM-ITGAX. *N. Engl. J. Med.*, **358**, 900–909.
12. Bottini, N., Musumeci, L., Alonso, A., Rahmouni, S., Nika, K., Rostamkhani, M., MacMurray, J., Meloni, G.F., Lucarelli, P., Pellecchia, M. *et al.* (2004) A functional variant of lymphoid tyrosine phosphatase is associated with type I diabetes. *Nat. Genet.*, **36**, 337–338.
13. Plenge, R.M., Cotsapas, C., Davies, L., Price, A.L., de Bakker, P.I., Maller, J., Pe'er, I., Burtt, N.P., Blumenstiel, B., DeFelice, M. *et al.* (2007) Two independent alleles at 6q23 associated with risk of rheumatoid arthritis. *Nat. Genet.*, **39**, 1477–1482.
14. Shimane, K., Kochi, Y., Yamada, R., Okada, Y., Suzuki, A., Miyatake, A., Kubo, M., Nakamura, Y. and Yamamoto, K. (2009) A single nucleotide polymorphism in the IRF5 promoter region is associated with susceptibility to rheumatoid arthritis in the Japanese population. *Ann. Rheum. Dis.*, **68**, 377–383.
15. Gateva, V., Sandling, J.K., Hom, G., Taylor, K.E., Chung, S.A., Sun, X., Ortmann, W., Kosoy, R., Ferreira, R.C., Nordmark, G. *et al.* (2009) A large-scale replication study identifies TNIP1, PRDM1, JAZF1, UHRF1BP1 and IL10 as risk loci for systemic lupus erythematosus. *Nat. Genet.*, **41**, 1228–1233.
16. Shao, H., Kono, D.H., Chen, L.Y., Rubin, E.M. and Kaye, J. (1997) Induction of the early growth response (Egr) family of transcription factors during thymic selection. *J. Exp. Med.*, **185**, 731–744.
17. Topilko, P., Schneider-Maunoury, S., Levi, G., Baron-Van Evercooren, A., Chennoufi, A.B., Seitanidou, T., Babinet, C. and Charnay, P. (1994) Krox-20 controls myelination in the peripheral nervous system. *Nature*, **371**, 796–799.
18. Decker, E.L., Skerka, C. and Zipfel, P.F. (1998) The early growth response protein (EGR-1) regulates interleukin-2 transcription by synergistic interaction with the nuclear factor of activated T cells. *J. Biol. Chem.*, **273**, 26923–26930.

19. Collins, S., Lutz, M.A., Zarek, P.E., Anders, R.A., Kersh, G.J. and Powell, J.D. (2008) Opposing regulation of T cell function by Egr-1/NAB2 and Egr-2/Egr-3. *Eur. J. Immunol.*, **38**, 528–536.
20. Zhu, B., Symonds, A.L., Martin, J.E., Kioussis, D., Wraith, D.C., Li, S. and Wang, P. (2008) Early growth response gene 2 (Egr-2) controls the self-tolerance of T cells and prevents the development of lupuslike autoimmune disease. *J. Exp. Med.*, **205**, 2295–2307.
21. Okamura, T., Fujio, K., Shibuya, M., Sumitomo, S., Shoda, H., Sakaguchi, S. and Yamamoto, K. (2009) CD4 + CD25-LAG3+ regulatory T cells controlled by the transcription factor Egr-2. *Proc. Natl Acad. Sci. USA*, **106**, 13974–13979.
22. Consortium, T.W.T.C.C. (2007) Genome-wide association study of 14,000 cases of seven common diseases and 3,000 shared controls. *Nature*, **447**, 661–678.
23. Rioux, J.D., Xavier, R.J., Taylor, K.D., Silverberg, M.S., Goyette, P., Huett, A., Green, T., Kuballa, P., Barmada, M.M., Datta, L.W. *et al.* (2007) Genome-wide association study identifies new susceptibility loci for Crohn disease and implicates autophagy in disease pathogenesis. *Nat. Genet.*, **39**, 596–604.
24. Ina, K., Itoh, J., Fukushima, K., Kusugami, K., Yamaguchi, T., Kyokane, K., Imada, A., Binion, D.G., Musso, A., West, G.A. *et al.* (1999) Resistance of Crohn's disease T cells to multiple apoptotic signals is associated with a Bcl-2/Bax mucosal imbalance. *J. Immunol.*, **163**, 1081–1090.
25. Brand, S. (2009) Crohn's disease: Th1, Th17 or both? The change of a paradigm: new immunological and genetic insights implicate Th17 cells in the pathogenesis of Crohn's disease. *Gut*, **58**, 1152–1167.
26. Newton, J.S., Li, J., Ning, Z.Q., Schoendorf, D.E., Norton, J.D. and Murphy, J.J. (1996) B cell early response gene expression coupled to B cell receptor, CD40 and interleukin-4 receptor co-stimulation: evidence for a role of the egr-2/krox 20 transcription factor in B cell proliferation. *Eur. J. Immunol.*, **26**, 811–816.
27. Mittelstadt, P.R. and Ashwell, J.D. (1999) Role of Egr-2 in up-regulation of Fas ligand in normal T cells and aberrant double-negative lpr and gld T cells. *J. Biol. Chem.*, **274**, 3222–3227.
28. Stranger, B.E., Nica, A.C., Forrest, M.S., Dimas, A., Bird, C.P., Beazley, C., Ingle, C.E., Dunning, M., Flicek, P., Koller, D. *et al.* (2007) Population genomics of human gene expression. *Nat. Genet.*, **39**, 1217–1224.
29. Suzuki, A., Yamada, R., Kochi, Y., Sawada, T., Okada, Y., Matsuda, K., Kamatani, Y., Mori, M., Shimane, K., Hirabayashi, Y. *et al.* (2008) Functional SNPs in CD244 increase the risk of rheumatoid arthritis in a Japanese population. *Nat. Genet.*, **40**, 1224–1229.
30. Begovich, A.B., Carlton, V.E., Honigberg, L.A., Schrodi, S.J., Chokkalingam, A.P., Alexander, H.C., Ardlie, K.G., Huang, Q., Smith, A.M., Spoerke, J.M. *et al.* (2004) A missense single-nucleotide polymorphism in a gene encoding a protein tyrosine phosphatase (PTPN22) is associated with rheumatoid arthritis. *Am. J. Hum. Genet.*, **75**, 330–337.
31. Vang, T., Congia, M., Macis, M.D., Musumeci, L., Orru, V., Zavattari, P., Nika, K., Tautz, L., Tasken, K., Cucca, F. *et al.* (2005) Autoimmune-associated lymphoid tyrosine phosphatase is a gain-of-function variant. *Nat. Genet.*, **37**, 1317–1319.
32. Hasegawa, K., Martin, F., Huang, G., Tumas, D., Diehl, L. and Chan, A.C. (2004) PEST domain-enriched tyrosine phosphatase (PEP) regulation of effector/memory T cells. *Science*, **303**, 685–689.
33. Lauritsen, J.P., Kurella, S., Lee, S.Y., Lefebvre, J.M., Rhodes, M., Alberola-Ila, J. and Wiest, D.L. (2008) Egr2 is required for Bcl-2 induction during positive selection. *J. Immunol.*, **181**, 7778–7785.
34. Strasser, A., Harris, A.W. and Cory, S. (1991) Bcl-2 transgene inhibits T cell death and perturbs thymic self-censorship. *Cell*, **67**, 889–899.
35. Kamatani, N., Kitamura, M.K.Y., Harigai, M., Okumoto, T. and Sumio, Y. (2004) Establishment of B-cell lines derived from 996 Japanese individuals. *Tissue Culture Research Communications*, **23**, 71–80.
36. Arnett, F.C., Edworthy, S.M., Bloch, D.A., McShane, D.J., Fries, J.F., Cooper, N.S., Healey, L.A., Kaplan, S.R., Liang, M.H., Luthra, H.S. *et al.* (1988) The American Rheumatism Association 1987 revised criteria for the classification of rheumatoid arthritis. *Arthritis Rheum.*, **31**, 315–324.
37. Andrews, N.C. and Faller, D.V. (1991) A rapid micropreparation technique for extraction of DNA-binding proteins from limiting numbers of mammalian cells. *Nucleic Acids Res.*, **19**, 2499.

# $CD4^+CD25^-LAG3^+$ regulatory T cells controlled by the transcription factor Egr-2

Tomohisa Okamura[a], Keishi Fujio[a,1], Mihoko Shibuya[a], Shuji Sumitomo[a], Hirofumi Shoda[a], Shimon Sakaguchi[b], and Kazuhiko Yamamoto[a]

[a]Department of Allergy and Rheumatology, Graduate School of Medicine, University of Tokyo, 7-3-1 Hongo, Bunkyo-ku, Tokyo 113-8655, Japan; and [b]Department of Experimental Pathology, Institute for Frontier Medical Sciences, Kyoto University, 53 Shogoin Kawahara-cho, Sakyo-ku, Kyoto 606-8507, Japan

Communicated by Tadatsugu Taniguchi, University of Tokyo, Tokyo, Japan, June 24, 2009 (received for review March 13, 2009)

**Regulatory T cells (Tregs) are engaged in the maintenance of immunological self-tolerance and immune homeostasis. IL-10 has an important role in maintaining the normal immune state. Here, we show that IL-10-secreting Tregs can be delineated in normal mice as $CD4^+CD25^-Foxp3^-$ T cells that express lymphocyte activation gene 3 (LAG-3), an MHC-class-II-binding CD4 homolog. Although ≈2% of the $CD4^+CD25^-$ T cell population consisted of $CD4^+CD25^-LAG3^+$ T cells in the spleen, $CD4^+CD25^-LAG3^+$ T cells are enriched to ≈8% in the Peyer's patch. They are hypoproliferative upon in vitro antigenic stimulation and suppress in vivo development of colitis. Gene expression analysis reveals that $CD4^+CD25^-LAG3^+$ Tregs characteristically express early growth response gene 2 (Egr-2), a key molecule for anergy induction. Retroviral gene transfer of Egr-2 converts naïve $CD4^+$ T cells into the IL-10-secreting and LAG-3-expressing phenotype, and Egr-2-transduced $CD4^+$ T cells exhibit antigen-specific immunosuppressive capacity in vivo. Unlike $Foxp3^+$ natural Tregs, high-affinity interactions with selecting peptide/MHC ligands expressed in the thymus do not induce the development of $CD4^+CD25^-LAG3^+$ Tregs. In contrast, the number of $CD4^+CD25^-LAG3^+$ Tregs is influenced by the presence of environmental microbiota. Thus, IL-10-secreting Egr-$2^+LAG3^+CD4^+$ Tregs can be exploited for the control of peripheral immunity.**

anergy | Blimp-1 | inflammatory bowel disease | IL-10 | type 1 regulatory T cells

Thymic T cell development efficiently regulates tolerance to self antigens (1, 2). However, in the last decade, rapid progress revealed the key role of peripheral tolerance in the maintenance of immunological homeostasis (3–5). In view of the recent reports, T cell subsets in the periphery are quite diverse. Naïve $CD4^+$ T helper cells may develop into different committed helper cell subsets characterized by distinct cytokine profiles, such as IFN-γ-secreting Th1, IL-4-secreting Th2, and IL-17-secreting Th17 cells (6–8). The versatile nature of T cells is found most strikingly in $Foxp3^+$ regulatory T cells (Tregs) (9). Therefore, identifying new subsets of effector and regulatory T cells is possible.

Naturally occurring $CD4^+CD25^+$ Tregs, which characteristically express the transcription factor Foxp3 (9), have been studied intensively, because their deficiency abrogates self-tolerance and causes autoimmune diseases (10). Mice with a null mutation of Foxp3, scurfy mice, have massive lymphoproliferation and severe inflammatory infiltration of the skin and liver (11). However, Aire is a gene responsible for autoimmune polyendocrinopathy–candidiasis–ectodermal dystrophy, which influences on the central induction of tolerance by regulating the clonal deletion of self-reactive thymocytes (12). Aire regulates the ectopic expression of a battery of peripheral-tissue antigens in the thymus [e.g., insulin, fatty-acid-binding protein, and salivary protein 1 (13)]. By an additional defect in central tolerance induction in scurfy mice, generated by crossing in a null mutation of the Aire gene, the range of affected sites was not noticeably extended, and many organs remained unaffected (3). This result suggests that additional important mechanisms other than central tolerance and the Foxp3 system are required to enforce immunological self-tolerance in the periphery.

Indeed, there are T cell populations with regulatory activity other than $CD4^+CD25^+Foxp3^+$ Tregs. The IL-10-secreting $Foxp3^-CD4^+$ T cells (4, 14) also have been a focus of active investigation, because, in contrast to $Foxp3^+$ natural Tregs, antigen-specific IL-10-secreting T cells can be adaptively induced in vitro and in vivo (15, 16). Because IL-10-secreting T cells also appear to be capable of controlling tissue inflammation under various disease conditions (14), IL-10-secreting regulatory T cells may be a tolerogenic machinery complementing $CD4^+CD25^+Foxp3^+$ Tregs. However, assessing the in vivo physiological function of IL-10-secreting regulatory T cells is difficult, because of the lack of specific markers that can reliably differentiate them from the other T cells (17).

Known regulatory T cells are closely related to anergy. Anergy is a tolerance mechanism in that T cells are functionally inactivated following an antigen encounter but remain alive for an extended period in the hyporesponsive state (18). A set of functional limitations characterizes the anergic state, including cell division, cell differentiation, and cytokine production. The E3 ligases c-Cbl, Cbl-b, GRAIL, Itch, and Nedd4 have been linked to the promotion of T cell anergy (19, 20). The RING-type E3 ubiquitin ligase Cbl-b promotes ubiquitination and degradation of signaling components, such as phospholipase C-γ and PKC-θ. Recently, early growth response gene 2 (Egr-2) and Egr-3 were reported to be transcription factors for the T cell receptor (TCR)-induced negative regulatory program controlling Cbl-b expression (21). Egr-2 is a C2H2-type zinc finger transcription factor that plays an essential role in hindbrain development and myelination of the peripheral nervous system (22), and Egr-2 null mutation resulted in perinatal or neonatal death. However, the role of Egr-2 in the regulatory function of T cells has not been described extensively.

We here report the identification of a Treg population that expresses Egr-2 and lymphocyte activation gene 3 (LAG-3). LAG-3, which negatively controls T cell proliferation (23, 24), was reported to be required for maximal regulatory functioning of murine $CD4^+CD25^+$ T cells. Ectopic expression of LAG-3 conferred regulatory activity to naïve T cells (25). Interestingly, LAG-3 protein was hardly detected on the cell surface of $CD4^+CD25^+$ T cells but was expressed by a sizable population of $CD4^+CD25^-$ T cells (26). We have found that IL-10-secreting $CD4^+CD25^-LAG3^+$ T cells show a significant regulatory activ-

Author contributions: T.O., K.F., S. Sakaguchi, and K.Y. designed research; T.O., K.F., M.S., S. Sumitomo, and H.S. performed research; T.O., K.F., S. Sakaguchi, and K.Y. analyzed data; and T.O., K.F., S. Sakaguchi, and K.Y. wrote the paper.

The authors declare no conflict of interest.

[1]To whom correspondence should be addressed. E-mail: kfujio-tky@umin.ac.jp.

This article contains supporting information online at www.pnas.org/cgi/content/full/0906872106/DCSupplemental.



www.pnas.org/cgi/doi/10.1073/pnas.0906872106

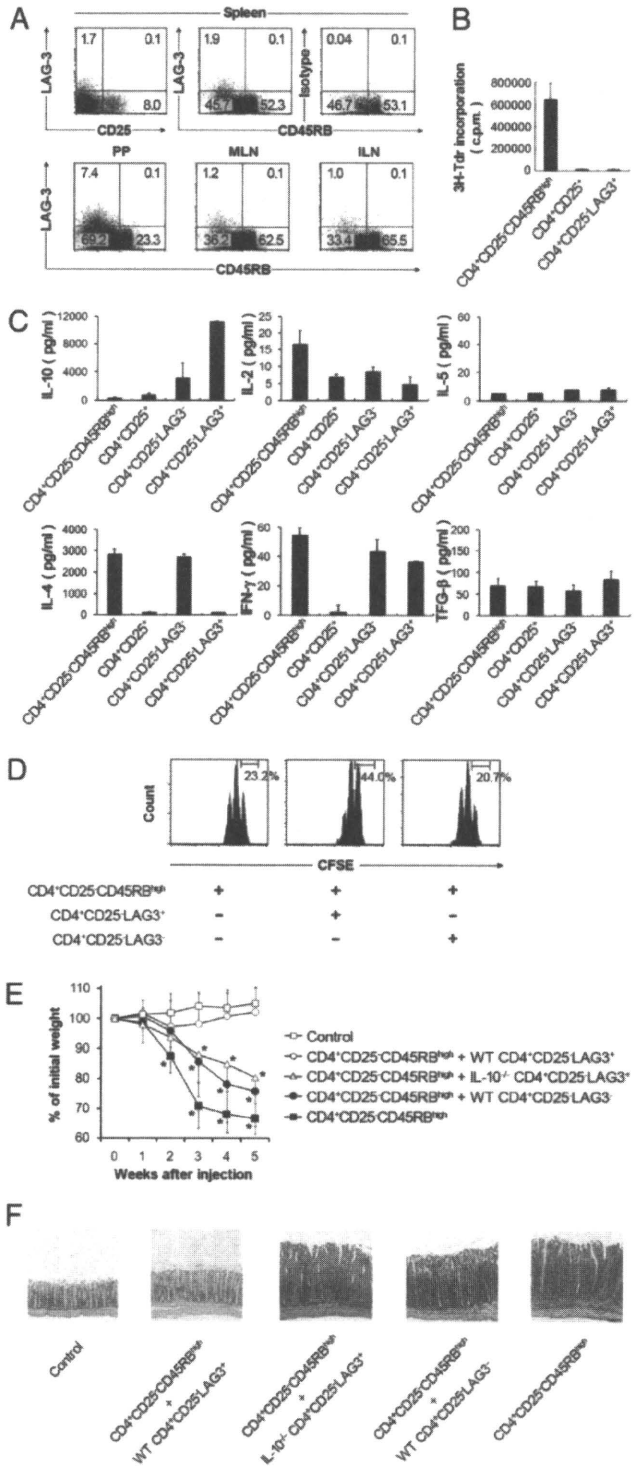


**Fig. 1.** Identification of $CD4^+CD25^-LAG3^+$ regulatory T cells. (*A*) LAG-3 expression in the spleen, Peyer's patch (PP), mesenteric lymph node (MLN), and inguinal lymph node (ILN). (*Top*) LAG-3 and CD25 or CD45RB expression in splenocytes from C57BL/6 is shown for the gated on $CD4^+$ (*Upper Left*) or $CD4^+CD25^-$ (*Upper Center* and *Upper Right*) T cells, respectively. (*Lower*) LAG-3 and CD45RB expression of PP, MLN, and ILN gated on $CD4^+CD25^-$ T cells. Representative FACS dot plots from at least three independent experiments are shown. (*B*) Proliferation of $CD4^+CD25^-CD45RB^{high}$, $CD4^+CD25^-$, and $CD4^+CD25^-LAG3^+$ splenocytes after 72 h stimulation with anti-CD3/anti-CD28. The results are the means of three independent experiments. (*C*) Cytokines in the culture supernatants of $CD4^+CD25^-CD45RB^{high}$, $CD4^+CD25^-$, and $CD4^+CD25^-LAG3^+$ T cells stimulated for 5 days with anti-CD3 mAb. Representative data from at least three independent experiments are shown. (*D*) Suppressive function of $CD4^+CD25^-LAG3^+$ T cells. Naïve $CD4^+CD25^-CD45RB^{high}$ $Thy1.1^+$ T cells were labeled with carboxyfluorescein diacetate succinimidyl ester (CFSE) and cocultured with the indicated $Thy1.2^+$ T cells and irradiated whole splenocytes plus anti-CD3 mAb. Representative data from three independent experiments are shown. (*E*) Suppression of $CD4^+CD25^-CD45RB^{high}$ T-cell-mediated colitis in RAG-$1^{-/-}$ mice by $CD4^+CD25^-LAG3^+$ T cells. Data represent body weight as a percentage of the initial weight of individual mice; $n = 6$ per group. (*F*) Representative photomicrographs of the colons stained with hematoxylin and eosin after transfer of the indicated cell populations. All error bars represent ±SD. (Scale bar, 100 μm.)

ity in vivo and characteristically express Egr-2. Conversion of Egr-2 transduced naïve $CD4^+$ T cells to IL-10-secreting and LAG-3-expressing Tregs suggested that Egr-2 is a key transcription factor for $CD4^+CD25^-LAG3^+$ T cells.

## Results

**IL-10-Secreting $CD4^+CD25^-CD45RB^{low}LAG3^+$ T Cells Exert Regulatory Activity.** In agreement with previous results (26), flow cytometric analysis revealed that >90% of LAG-3-expressing cells belonged to the $CD4^+CD25^-CD45RB^{low}$ population (hereafter called $CD4^+CD25^-LAG3^+$ cells) (Fig. 1*A*). These $CD4^+CD25^-LAG3^+$ cells showed staining profiles of conventional $CD4^-TCR\alpha\beta^+$ T cells that did not express CD8, TCRγδ, and NK1.1 antigens (Fig. S1). The frequencies of $LAG3^+$ T cells in the $CD4^+CD25^-$ population were relatively low in the spleen (1.8 ± 0.18%), mesenteric lymph node (1.1 ± 0.09%), and inguinal lymph node (1.0 ± 0.07%) but characteristically high in Peyer's patch (PP) (7.7 ± 0.87%). These cells were hypoproliferative upon in vitro stimulation in a manner similar to $CD4^+CD25^+$ Tregs (Fig. 1*B*). They exclusively produced large amounts of IL-10 and low amounts of IL-2 and IL-4 (Fig. 1*C*). There were no significant differences in IL-5 and TGF-β production among the populations compared in the experiment. In anti-CD3-stimulated cocultures of $LAG3^+$ or $LAG3^-CD4^+CD25^-$ T cells with $CD4^+CD25^-CD45RB^{high}$ T cells, $CD4^+CD25^-LAG3^+$ T cells exhibited weak suppressive activity (Fig. 1*D*). In contrast, $CD4^-CD25^-LAG3^+$ T cells effectively inhibited colitis induced in RAG-1-deficient (RAG-$1^{-/-}$) recipients by the transfer of $CD4^+CD25^-CD45RB^{high}$ T cells (Fig. 1 *E* and *F* and Fig. S2). The in vivo suppressive activity was IL-10-dependent, because the transfer of $CD4^+CD25^-LAG3^+$ T cells from congenic IL-10-deficient (IL-$10^{-/-}$) mice failed to suppress colitis.

Cytofluorometric analysis revealed that $CD4^+CD25^-LAG3^+$ T cells did not express Foxp3 protein (Fig. S3 and Fig. S4). In addition, the number of $CD4^+CD25^-LAG3^+$ T cells was significantly increased in scurfy mice that lack functional Foxp3 protein (11). These cells expressed LAG-3 and IL-10 mRNA equivalently and exhibited distinct in vitro suppressive activity (Fig. S5). $CD4^+CD25^-LAG3^+$ T cells hardly expressed CD103 and latency-associated peptide (LAP) on the cell surface (Fig. S1 and Fig. S6), indicating that they were different from $CD103^+$ regulatory T cells and $CD4^+CD25^-LAP^+$ regulatory T cells, respectively (27, 28). These findings collectively indicate that $CD4^+CD25^-LAG3^+$ T cells exert regulatory activity in an IL-10-dependent and Foxp3-independent manner.

**$CD4^+CD25^-CD45RB^{low}LAG3^+$ T Cells Exhibit a Distinct Transcriptional Profile.** To further characterize $CD4^+CD25^-LAG3^+$ T cells, the mRNA expression profiles of four $CD4^+$ subsets ($CD4^+CD25^-LAG3^+$, $CD4^+CD25^-LAG3^-$, $CD4^+CD25^+$, and $CD4^+CD25^-CD45RB^{high}$) were examined. Gene expression profiling revealed six clusters of differentially expressed genes

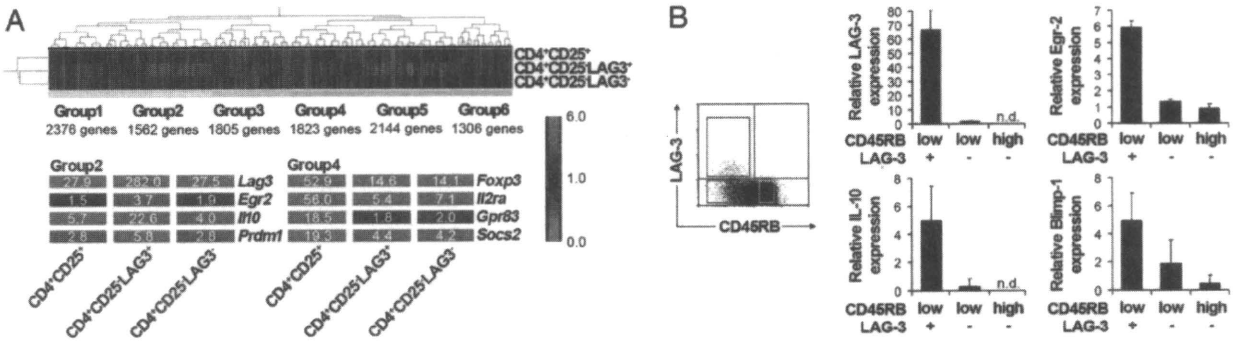


**Fig. 2.** Expression of Egr-2 in CD4$^-$CD25$^-$LAG3$^+$ T cells confers regulatory function. (*A*) Microarray comparisons of the gene expression profiles among CD4$^-$CD25$^+$, CD4$^+$CD25$^-$ LAG3$^+$, and CD4$^+$CD25$^-$LAG3$^-$ cells. Normalized expression values from naïve CD4$^+$CD25$^-$ CD45RB$^{high}$ T cells are depicted according to the color scale shown. The expression profiles for each gene were classified into six groups. (*B*) LAG-3 and CD45RB expression of splenocytes from C57BL/6 mice gated-on CD4$^+$CD25$^-$ T cells (*Left*). Quantitative PCR for LAG-3, Egr-2, IL-10, and Blimp-1 in the indicated T cell subsets (*Right*). The results are the means of three independent experiments. All error bars represent ±SD.

(Fig. 2*A*). Signature genes for CD4$^+$CD25$^+$ Tregs, such as *Foxp3*, *Il2ra* (CD25), *Gpr83*, and *Socs2*, were preferentially expressed in one group (group 4). In contrast, the supposed signature genes for CD4$^+$CD25$^-$LAG3$^-$, such as *Lag3*, *Il10*, and *Prdm1* [B-lymphocyte-induced maturation protein 1 (Blimp-1)], were preferentially expressed in another group (group 2). Because CD4$^+$CD25$^-$LAG3$^+$ T cells were anergic in response to TCR stimulation (Fig. 1*B*), that the expression of the anergy-associated Egr2 gene was significantly increased in group 2 is particularly notable. Egr-2 was reported recently as a key negative regulator of T cell activation and was required for full induction of clonal anergy (21, 29). In accordance with the microarray analysis, quantitative real-time PCR confirmed the high expression levels of Egr2, LAG3, IL-10, and Blimp-1 genes in CD4$^+$CD25$^-$LAG3$^+$ T cells (Fig. 2*B*).

**Retroviral Transduction of Egr-2 Converts Naïve CD4$^+$ T Cells into IL-10-Secreting and LAG-3-Expressing Tregs.** Next, we examined whether forced expression of Egr-2 in naïve CD4$^+$ T cells could convert them to the CD4$^+$CD25$^-$LAG3$^+$ phenotype using retrovirus vectors that coexpressed GFP and Egr-2 (pMIG-Egr2) (Fig. 3*A*). The TCR-stimulated pMIG-Egr2-transduced GFP$^+$ cells showed significant up-regulation of Egr2, LAG3, IL-10, and Blimp-1 genes (Fig. 3*B*). In addition, pMIG-Egr2-transduced GFP$^+$ cells produced significantly higher amounts of IL-10 and lower amounts of IL-2, IL-4, and IL-5 proteins (Fig. 3*C*).

Despite the expression of LAG-3 and IL-10 proteins, the present study was not able to confirm sufficient suppressive activity of pMIG-Egr2-transduced GFP$^+$ cells in in vitro coculture with freshly isolated CD4$^+$CD25$^-$CD45RB$^{high}$ responder T cells stimulated with anti-CD3 mAb (Fig. 3*D*). To examine the in vivo suppressive activity of Egr-2, we next performed the delayed-type hypersensitivity (DTH) reaction of BALB/c mice against chicken ovalbumin (OVA) by using T cells transduced with the Egr2 gene. The in vivo functions of T cells transduced with regulatory genes have been verified (30, 31). In this experiment, CD4$^+$ T cells from BALB/c mice were transduced with pMIG or pMIG-Egr2. FACS-sorted retrovirus-infected CD4$^+$GFP$^+$ cells were injected intravenously 6 days after immunization with OVA, and OVA was rechallenged 2 days after the cell transfer. Notably, BALB/c CD4$^+$ T cells transduced with pMIG-Egr2 significantly suppressed DTH responses compared with BALB/c CD4$^+$ T cells transduced with pMIG (Fig. 3*E*). To explore the influence of antigen specificity, CD4$^+$ T cells from OVA-specific DO11.10 TCR transgenic mice also were transduced with pMIG or pMIG-Egr2, and mice transferred with these CD4$^+$GFP$^+$ cells were simultaneously analyzed for DTH. DO11.10 CD4$^+$ T cells transduced with pMIG-Egr2 significantly suppressed DTH responses compared with BALB/c CD4$^+$ T cells transduced with pMIG. Moreover, DO11.10 CD4$^+$ T cells transduced with pMIG-Egr2 suppressed DTH responses more efficiently than BALB/c CD4$^+$ T cells transduced with pMIG-Egr2, indicating a contribution of the antigen specificity to the enhancement of suppressive activity in Egr2-transduced cells. Thus, Egr-2 can confer in vivo suppressive activity on naïve T cells.

**Development of CD4$^+$CD25$^-$LAG3$^+$ T Cells.** We then explored whether CD4$^+$CD25$^-$LAG3$^+$ T cells could develop through the thymic selection process in a similar manner to Foxp3$^+$ Tregs, which require a high-affinity agonistic interaction with self-peptide/MHCs expressed by thymic stromal cells (32). RIP-mOVA/OT-II double-transgenic mice express a membrane-bound form of OVA in the pancreatic islets and the thymus together with a transgenic TCR (V$\alpha$2 and V$\beta$5.1) that recognizes the $OVA_{323-339}$ peptide in the context of I-A$^b$. The frequency of CD4$^+$CD25$^-$LAG3$^+$ T cells was not increased in the thymus and spleen of RIP-mOVA/OT-II mice, in contrast with an increase in the frequency of CD4$^+$CD25$^+$ Tregs in these organs as reported in ref. 32 (Fig. 4*A*). Thus, unlike Foxp3$^+$ natural Tregs, the development of CD4$^+$CD25$^-$LAG3$^+$ T cells does not appear to require high-affinity interactions with selecting peptide/MHC ligands expressed in the thymus.

Next, the influence of the environmental microbiota was studied for the development of CD4$^+$CD25$^-$LAG3$^+$ T cells with germfree (GF) mice. Although GF mice are exposed to self antigens, to food-derived antigens, and to microbial particles from dead microorganisms in the sterilized food or bedding, the absence of viable microbiota affects the immune homeostasis (33, 34). As shown in Fig. 4*B*, GF mice contained fewer CD4$^+$CD25$^-$LAG3$^+$ T cells than specific-pathogen-free mice in the spleen and PP. This result suggested that the exposure to viable microbiota affects the development of CD4$^+$CD25$^-$LAG3$^+$ T cells.

## Discussion

We have shown the natural presence of Egr-2-dependent CD4$^+$CD25$^-$ Tregs in the normal immune system and characterized their function and development. CD4$^+$CD25$^-$LAG3$^+$ Tregs are clearly different from CD4$^+$CD25$^+$ Tregs in Foxp3 independency and development. T-cell-mediated colitis driven by enteric bacteria develops in lymphopenic mice after the transfer of CD4$^+$CD45RB$^{high}$ T cells (35). The development of colitis can be prevented by cotransfer of the reciprocal

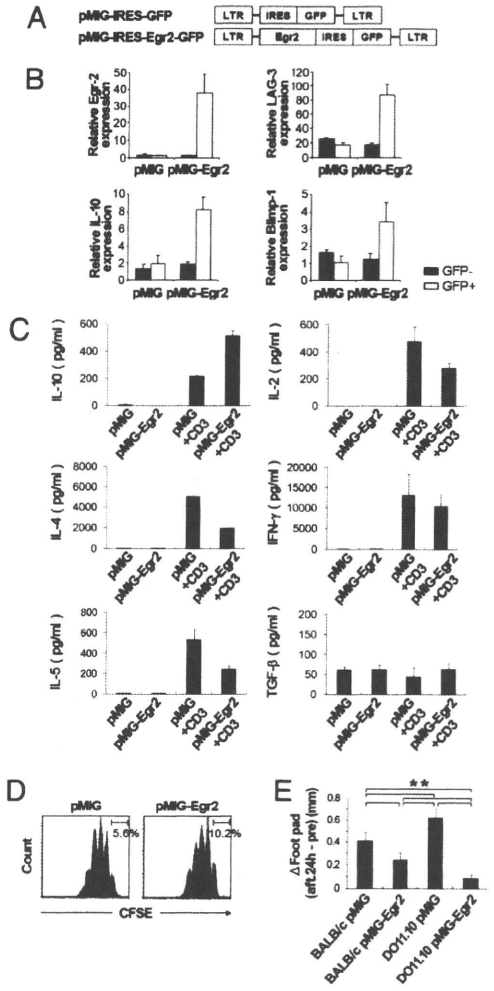


**Fig. 3.** Retroviral transduction of Egr-2 into naïve T cells. (*A*) Retroviral constructs for the transduction of Egr-2. (*B*) Ectopic Egr-2 expression induced the expression of LAG-3, IL-10, and Blimp-1. Quantitative PCR analyses of gene expression in sorted retrovirally transduced cell populations stimulated for 5 days with soluble anti-CD3 mAb (1 μg/mL). The results are the means of three independent experiments. (*C*) Cytokines in the culture supernatants of pMIG- and pMIG-Egr2-transduced $CD4^+GFP^+$ T cells stimulated for 48 h with or without plate-coated anti-CD3 mAb. The results are the means of three independent experiments. (*D*) Suppression of naïve carboxyfluorescein diacetate succinimidyl ester (CFSE)-labeled $CD4^+CD25^-CD45RB^{high}$ T cells by Egr-2-transduced T cells in vitro. Naïve $CD4^+CD25^-CD45RB^{high}$ $Thy1.1^+$ T cells were labeled with CFSE and cultured with the indicated retrovirally transduced $Thy1.2^-$ T cells and irradiated whole splenocytes plus anti-CD3 mAb. Representative data from three independent experiments are shown. (*E*) Antigen-specific suppression of the delayed-type hypersensitivity (DTH) response by Egr2-transduced $CD4^+$ T cells. Six days after primary immunization, FACS-sorted pMIG- or pMIG-Egr2-transduced $CD4^+$ T cells ($1 \times 10^6$) from BALB/c or DO11.10 mice were transferred adoptively via i.v. injection into BALB/c mice. Two days after adoptive cell transfer, DTH response in the footpad was induced. Footpad thickness was determined 24 h later; $n = 6$ per group. All error bars represent ±SD. **, $P < 0.01$.

$CD4^+CD45RB^{low}$ subset in an IL-10-dependent manner (36). The suppressive activity was independent of $CD4^+CD25^+$ Tregs, because $CD4^+CD25^+$ T-cell-depleted $CD4^+CD25^-CD45RB^{low}$ T cells retained suppressive activity (37). The present findings that $CD4^+CD25^-CD45RB^{low}LAG3^+$ T cells exhibited stronger suppressive activity than $CD4^+CD25^-CD45RB^{low}LAG3^-$ T cells indicated that the suppressive activity of $CD4^+CD25^-CD45RB^{low}$ T cells was confined mainly to $CD4^+CD25^-CD45RB^{low}LAG3^-$ T cells expressing high levels of Egr-2. The association between LAG-3 and IL-10 production was consistent with previous observations (25). In addition to $CD4^+CD25^-CD45RB^{low}$ T cells, a decade of active research has focused on IL-10-producing type 1 regulatory T cells (Tr1) induced in vitro by antigenic stimulation (14). $CD4^+CD25^-LAG3^+$ Tregs were probably different from Tr1 in that $CD4^+CD25^-LAG3^+$ Tregs did not produce TGF-β and IL-5 (14). However, the precise relationships between $CD4^+CD25^-LAG3^+$ Tregs and Tr1 should be investigated further, because an optimal stimulation may induce TGF-β and IL-5 production in $CD4^+CD25^-LAG3^+$ Tregs.

In this study, the suppressive phenotype of $CD4^+CD25^-LAG3^+$ Tregs was determined by Egr-2. Egr-2 transduced T cells exhibited antigen-specific immunosuppressive capacity in vivo. Forced expression of Egr-2 in $CD4^+$ T cells induced the expression of LAG3, IL-10, and Blimp-1 genes. These results are consistent with the recent findings that T-cell-specific Blimp-1 conditional knockout mice showed impaired IL-10 production and increased IL-2 production in activated $CD4^+$ T cells and that they developed spontaneous colitis (38, 39).

The extrathymic development of IL-10-secreting T cells already has been reported (40). The severe decrease of $CD4^+CD25^-LAG3^+$ Tregs in GF mice shows the importance of environmental microbiota for the development of $CD4^+CD25^-LAG3^+$ Tregs. Germfree models represent an important tool for uncovering the function of gut microbiota, especially their effects on mucosal immunity (33, 34). Recently, gut-associated lymphoid tissue has been demonstrated to be a preferential site for the peripheral induction of $Foxp3^+$ regulatory T cells (41). In particular, dendritic cells (DCs) expressing $CD103^+$ from the lamina propria of the small intestine and from the mesenteric lymph node can induce $Foxp3^+$ T cells (42). Plasmacytoid DCs presenting dietary antigens are responsible for induction of oral tolerance and immune suppression affecting both $CD4^+$ and $CD8^-$ responses (43). The precise mechanisms of the development of $CD4^-CD25^-LAG3^+$ Tregs by environmental microbiota and antigen-presenting cells should be examined further.

Recent genome-wide association studies reported SNPs on chromosome 10q21 with a strong association to Crohn's disease (44, 45), a common form of chronic inflammatory bowel disease (IBD). The associated intergenic region is flanked by Egr-2, suggesting that this genetic variation could regulate Egr-2 expression. The characteristically high production level of IL-10 by Egr-2-dependent $CD4^+CD25^-$ T cells suggests that this Treg population may contribute to the control of organ inflammation. Moreover, T-cell-specific Egr-2-deficient mice showed autoimmune disease characterized by the enhanced expression of proinflammatory cytokines and massive infiltration of T cells into multiple organs (46). By exploiting the capacity of Egr-2-dependent $CD4^+CD25^-LAG3^+$ Tregs to produce a large amount of IL-10, they can be useful for antigen-specific treatment of inflammatory disease, in particular IBD.

## Materials and Methods

**Mice.** BALB/c and C57BL/6 mice were purchased from Japan SLC. C57BL/6 recombinase-activating gene 1 (*rag-1*) deficient ($RAG1^{-/-}$) mice and TCR transgenic OT-II mice were purchased from Taconic. $RAG1^{-/-}$ mice were housed in microisolator cages with sterile filtered air. TCR transgenic DO11.10 mice, IL-10-deficient ($IL\text{-}10^{-/-}$) mice (47), B6.Thy1.1 mice, and Foxp3-eGFP mice (48) were purchased from Jackson Laboratory. RIP-mOVA (49) mice and B6.$Foxp3^{sf/+}$ female mice were purchased from Jackson Laboratory and backcrossed with C57BL/6 males. B6.$Foxp3^{sf/Y}$ male mice (11) were used at 21 days of age. All mice except B6.$Foxp3^{sf/Y}$ and B6.$Foxp3^{sf/+}$ were used at >7 weeks of age. All animal experiments were conducted in accordance with institutional and national guidelines.

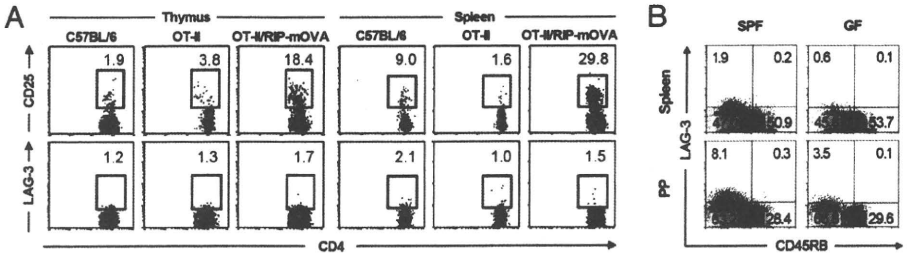


**Fig. 4.** Development of CD4$^+$CD25$^-$LAG3$^-$ T cells. (*A*) Flow cytometry of LAG-3 and CD25 expression in the thymus and spleen of OT-II TCR transgenic mice with or without the RIP-mOVA transgene. *Upper* and *Lower* plots are gated on CD4$^+$V$\beta$5.1/5.2$^+$ and CD4$^-$CD25$^-$V$\beta$5.1/5.2$^+$ T cells, respectively. Representative FACS dot plots from three independent experiments are shown. (*B*) Flow cytometry of LAG-3 and CD45RB expression in the spleen and Peyer's patch (PP) of specific-pathogen-free (SPF) (*Left*) and germfree (GF) (*Right*) mice gated on CD4$^+$CD25$^-$ T cells. Representative FACS dot plots from at least three independent experiments are shown.

**Reagents.** Purified and conjugated antibodies were purchased from BD Pharmingen, eBioscience, or Miltenyi Biotec, and recombinant cytokines were obtained from R&D Systems. See *SI Materials and Methods* for details.

**RNA Isolation, cDNA Synthesis, and Quantitative Real-Time PCR.** Total T cell RNA was prepared using an RNeasy Micro Kit (Qiagen). RNA was reverse-transcribed to cDNA, and quantitative real-time PCR analysis was performed as described in *SI Materials and Methods*. Relative RNA abundance was determined based on control $\beta$-actin abundance.

**DNA Microarray Analysis.** Total RNA of CD4$^+$CD25$^+$, CD4$^+$CD25$^-$CD45RB$^{low}$LAG3$^+$, CD4$^+$CD25$^-$CD45RB$^{low}$LAG3$^-$, and CD4$^+$CD25$^-$CD45RB$^{high}$ FACS-purified T cells from C57BL/6 mice were harvested as described above and then prepared for Affymetrix microarray analysis as described in *SI Materials and Methods*. The data were analyzed using Bioconductor (version 1.9) (50) statistical software R and GeneSpring GX version 7.3.1 (Silicon Genetics). All microarray data have been deposited in the ArrayExpress database (http://www.ebi.ac.uk/arrayexpress) under accession number E-MEXP-1343.

**Proliferation Assay.** Each T cell population ($1 \times 10^5$ cells per well) purified from C57BL/6 mice was cultured in U-bottomed 96-well plates coated anti-CD3 mAb for 72 h. $^3$H-thymidine (1 $\mu$Ci per well; NEN Life Science Products) was added during the last 15 h of culture. Cells were harvested and counted using a $\beta^-$ counter. Results were expressed as the mean $\pm$ SD of triplicate cultures.

**Suppression Assay.** FACS-purified CD4$^+$CD25$^-$CD45RB$^{high}$ T cells isolated from B6.Thy1.1 mice were stained with 5 $\mu$M carboxyfluorescein diacetate succinimidyl ester (CFSE) by incubating them for 10 min at 37 °C. The reaction was quenched by washing in ice-cold RPMI medium 1640 supplemented with 10% FCS. The CFSE-labeled CD4$^+$CD25$^-$CD45RB$^{high}$ T cells ($5 \times 10^4$) were cocultured with $1 \times 10^5$ irradiated whole splenocytes in the presence or absence of $5 \times 10^4$ retrovirally gene-transduced CD4$^+$GFP$^+$-sorted T cells or CD4$^-$CD25$^-$CD45RB$^{low}$LAG3$^{+\ or-}$ T cells from C57BL/6 mice in U-bottomed 96-well plates in the presence of 1.0 $\mu$g/mL anti-CD3 mAb. After 72 h, cells were analyzed by flow cytometry and gated on Thy1.1$^+$CD4$^+$ cells.

**Colitis Model.** Syngenic purified CD4$^+$CD25$^-$CD45RB$^{high}$ T cells ($1 \times 10^5$), described above, from C57BL/6 mice were injected i.p. into RAG1$^{-/-}$ mice alone or in combination with $1 \times 10^5$ wild-type CD4$^+$CD25$^-$CD45RB$^{low}$LAG3$^{+\ or-}$ or IL-10$^{-/-}$ CD4$^+$CD25$^-$CD45RB$^{low}$LAG3$^+$ T cells. Control mice received PBS. Mice were observed daily and weighed weekly. Seven weeks after cell transfer, the mice were killed, and sections of the colons were stained with hematoxylin and eosin. Mice were killed to assess the severity of colitis as described in *SI Materials and Methods*.

**Cytokine Detection.** Supernatants from cultures of CD4$^+$ T cells untreated or stimulated by plate-bound anti-CD3 (5 $\mu$g/mL) for 48 h or 5 days were harvested and pooled, and IL-2, IL-4, IL-5, IL-10, IFN-$\gamma$, and TGF-$\beta$ concentrations were measured using a commercially available LINCOplex Mouse Cytokine kit (Linco Research) using fluorescently labeled microsphere beads and a Luminex reader according to the manufacturer's instructions at GeneticLabo. Raw data (mean fluorescence intensities) from the beads were analyzed using MasterPlex QT version 2.5 software (Hitachi) to obtain concentration values. All samples were run in duplicate, and results were obtained three times.

**DTH Assay.** BALB/c mice were immunized with OVA 6 days before the transfer of gene-transduced T cells. Retroviral gene transduction to CD4$^+$ T cells has been reported (51). The experimental groups consisted of CD4$^+$ T cells from BALB/c or DO11.10 mice transduced with pMIG or pMIG-Egr2. In accordance with our previous experiments (30, 31), the average transduction efficiency was $\approx$50%. The GFP-positive fraction of the transduced CD4$^+$ T cells were sorted with FACSAria and transferred to immunized mice. OVA was rechallenged to the footpad 2 days after the transfer, and footpad swelling was measured 24 h later. Detailed protocols are described in *SI Materials and Methods*.

**Statistical Analysis.** Statistical significance was analyzed using Statview software (SAS Institute). Body weight changes were analyzed by repeated measures two-way ANOVA followed by Bonferroni post test. Colitis scores, quantitative histology, and DTH responses were analyzed with the Mann–Whitney, Scheffé, and Bonferroni tests, respectively. Differences were considered statistically significant with *, $P < 0.05$ and **, $P < 0.01$.

**ACKNOWLEDGMENTS.** We thank K. Watada for excellent technical assistance. Flow cytometry analysis and cell sorting were done in the Department of Transfusion Medicine and Immunohematology, University of Tokyo, Japan. This work was supported by grants from the Japan Society for the Promotion of Science, Ministry of Health, Labor and Welfare, and the Ministry of Education, Culture, Sports, Science and Technology (MEXT) (in part by Global COE Program Chemical Biology of the Diseases, by the MEXT), Japan.

1. Starr TK, Jameson SC, Hogquist KA (2003) Positive and negative selection of T cells. *Annu Rev Immunol* 21:139–176.
2. Hogquist KA, Baldwin TA, Jameson SC (2005) Central tolerance: Learning self-control in the thymus. *Nat Rev Immunol* 5:772–782.
3. Chen Z, Benoist C, Mathis D (2005) How defects in central tolerance impinge on a deficiency in regulatory T cells. *Proc Natl Acad Sci USA* 102:14735–14740.
4. Roncarolo MG, et al. (2006) Interleukin-10-secreting type 1 regulatory T cells in rodents and humans. *Immunol Rev* 212:28–50.
5. Fife BT, Bluestone JA (2008) Control of peripheral T-cell tolerance and autoimmunity via the CTLA-4 and PD-1 pathways. *Immunol Rev* 224:166–182.
6. Kalinski P, Moser M (2005) Consensual immunity: Success-driven development of T-helper-1 and T-helper-2 responses. *Nat Rev Immunol* 5:251–260.
7. Kano S, et al. (2008) The contribution of transcription factor IRF1 to the interferon-$\gamma$–interleukin 12 signaling axis and $T_H1$ versus $T_H$-17 differentiation of CD4$^+$ T cells. *Nat Immunol* 9:34–41.
8. Dong C (2008) TH17 cells in development: An updated view of their molecular identity and genetic programming. *Nat Rev Immunol* 8:337–348.
9. Hori S, Nomura T, Sakaguchi S (2003) Control of regulatory T cell development by the transcription factor Foxp3. *Science* 299:1057–1061.
10. Sakaguchi S, Powrie F (2007) Emerging challenges in regulatory T cell function and biology. *Science* 317:627–629.
11. Brunkow ME, et al. (2001) Disruption of a new forkhead/winged-helix protein, scurfin, results in the fatal lymphoproliferative disorder of the scurfy mouse. *Nat Genet* 27:68–73.
12. Liston A, Lesage S, Wilson J, Peltonen L, Goodnow CC (2003) Aire regulates negative selection of organ-specific T cells. *Nat Immunol* 4:350–354.
13. Anderson MS, et al. (2005) The cellular mechanism of Aire control of T cell tolerance. *Immunity* 23:227–239.
14. Groux H, et al. (1997) A CD4$^+$ T-cell subset inhibits antigen-specific T-cell responses and prevents colitis. *Nature* 389:737–742.

15. Barrat FJ, et al. (2002) In vitro generation of interleukin 10-producing regulatory CD4$^-$ T cells is induced by immunosuppressive drugs and inhibited by T helper type 1 (Th1)- and Th2-inducing cytokines. *J Exp Med* 195:603–616.
16. Battaglia M, Gregori S, Bacchetta R, Roncarolo MG (2006) Tr1 cells: From discovery to their clinical application. *Semin Immunol* 18:120–127.
17. Roncarolo MG, Battaglia M (2007) Regulatory T-cell immunotherapy for tolerance to self antigens and alloantigens in humans. *Nat Rev Immunol* 7:585–598.
18. Schwartz RH (2003) T cell anergy. *Annu Rev Immunol* 21:305–334.
19. Mueller DL (2004) E3 ubiquitin ligases as T cell anergy factors. *Nat Immunol* 5:883–890.
20. Heissmeyer V, et al. (2004) Calcineurin imposes T cell unresponsiveness through targeted proteolysis of signaling proteins. *Nat Immunol* 5:255–265.
21. Safford M, et al. (2005) Egr-2 and Egr-3 are negative regulators of T cell activation. *Nat Immunol* 6:472–480.
22. Topilko P, et al. (1994) Krox-20 controls myelination in the peripheral nervous system. *Nature* 371:796–799.
23. Workman CJ, Vignali DA (2003) The CD4-related molecule, LAG-3 (CD223), regulates the expansion of activated T cells. *Eur J Immunol* 33:970–979.
24. Workman CJ, et al. (2004) Lymphocyte activation gene-3 (CD223) regulates the size of the expanding T cell population following antigen activation in vivo. *J Immunol* 172:5450–5455.
25. Huang CT, et al. (2004) Role of LAG-3 in regulatory T cells. *Immunity* 21:503–513.
26. Workman CJ, Rice DS, Dugger KJ, Kurschner C, Vignali DA (2002) Phenotypic analysis of the murine CD4-related glycoprotein, CD223 (LAG-3). *Eur J Immunol* 32:2255–2263.
27. Lehmann J, et al. (2002) Expression of the integrin $\alpha_E\beta_7$ identifies unique subsets of CD25$^-$ as well as CD25$^-$ regulatory T cells. *Proc Natl Acad Sci USA* 99:13031–13036.
28. Ochi H, et al. (2006) Oral CD3-specific antibody suppresses autoimmune encephalomyelitis by inducing CD4$^+$CD25$^-$LAP$^+$ T cells. *Nat Med* 12:627–635.
29. Harris JE, et al. (2004) Early growth response gene-2, a zinc-finger transcription factor, is required for full induction of clonal anergy in CD4$^+$ T cells. *J Immunol* 173:7331–7338.
30. Fujio K, et al. (2004) Nucleosome-specific regulatory T cells engineered by triple gene transfer suppress a systemic autoimmune disease. *J Immunol* 173:2118–2125.
31. Fujio K, et al. (2006) Gene therapy of arthritis with TCR isolated from the inflamed paw. *J Immunol* 177:8140–8147.
32. Coutinho A, Caramalho I, Seixas E, Demengeot J (2005) Thymic commitment of regulatory T cells is a pathway of TCR-dependent selection that isolates repertoires undergoing positive or negative selection. *Curr Top Microbiol Immunol* 293:43–71.
33. Tlaskalova-Hogenova H, et al. (2004) Commensal bacteria (normal microflora), mucosal immunity and chronic inflammatory and autoimmune diseases. *Immunol Lett* 93:97–108.
34. Wen L, et al. (2008) Innate immunity and intestinal microbiota in the development of type 1 diabetes. *Nature* 455:1109–1113.
35. Aranda R, et al. (1997) Analysis of intestinal lymphocytes in mouse colitis mediated by transfer of CD4$^+$, CD45RB$^{high}$ T cells to SCID recipients. *J Immunol* 158:3464–3473.
36. Asseman C, Mauze S, Leach MW, Coffman RL, Powrie F (1999) An essential role for interleukin 10 in the function of regulatory T cells that inhibit intestinal inflammation. *J Exp Med* 190:995–1004.
37. Annacker O, et al. (2001) CD25$^+$ CD4$^+$ T cells regulate the expansion of peripheral CD4 T cells through the production of IL-10. *J Immunol* 166:3008–3018.
38. Kallies A, et al. (2006) Transcriptional repressor Blimp-1 is essential for T cell homeostasis and self-tolerance. *Nat Immunol* 7:466–474.
39. Martins GA, et al. (2006) Transcriptional repressor Blimp-1 regulates T cell homeostasis and function. *Nat Immunol* 7:457–465.
40. Maynard CL, et al. (2007) Regulatory T cells expressing interleukin 10 develop from Foxp3$^+$ and Foxp3$^-$ precursor cells in the absence of interleukin 10. *Nat Immunol* 8:931–941.
41. Belkaid Y, Oldenhove G (2008) Tuning microenvironments: Induction of regulatory T cells by dendritic cells. *Immunity* 29:362–371.
42. Coombes JL, et al. (2007) A functionally specialized population of mucosal CD103$^+$ DCs induces Foxp3+ regulatory T cells via a TGF-$\beta$- and retinoic acid-dependent mechanism. *J Exp Med* 204:1757–1764.
43. Goubier A, et al. (2008) Plasmacytoid dendritic cells mediate oral tolerance. *Immunity* 29:464–475.
44. Rioux JD, et al. (2007) Genome-wide association study identifies new susceptibility loci for Crohn disease and implicates autophagy in disease pathogenesis. *Nat Genet* 39:596–604.
45. Wellcome Trust Case Control Consortium (2007) Genome-wide association study of 14,000 cases of seven common diseases and 3,000 shared controls. *Nature* 447:661–678.
46. Zhu B, et al. (2008) Early growth response gene 2 (Egr-2) controls the self-tolerance of T cells and prevents the development of lupuslike autoimmune disease. *J Exp Med* 205:2295–2307.
47. Berg DJ, et al. (1996) Enterocolitis and colon cancer in interleukin-10-deficient mice are associated with aberrant cytokine production and CD4$^+$ TH1-like responses. *J Clin Invest* 98:1010–1020.
48. Haribhai D, et al. (2007) Regulatory T cells dynamically control the primary immune response to foreign antigen. *J Immunol* 178:2961–2972.
49. Kurts C, et al. (1996) Constitutive class I-restricted exogenous presentation of self antigens in vivo. *J Exp Med* 184:923–930.
50. Gentleman RC, et al. (2004) Bioconductor: Open software development for computational biology and bioinformatics. *Genome Biol* 5:R80.
51. Fujio K, et al. (2000) Functional reconstitution of class II MHC-restricted T cell immunity mediated by retroviral transfer of the $\alpha\beta$ TCR complex. *J Immunol* 165:528–532.

The Journal of Toxicological Sciences (J. Toxicol. Sci.)
Vol.34, Special Issue II, SP349-SP361, 2009



# Children's Immunology, what can we learn from animal studies (3): Impaired mucosal immunity in the gut by 2,3,7,8-tetraclorodibenzo-p-dioxin (TCDD): A possible role for allergic sensitization

**Sho Ishikawa**

*Dept. of Molecular Preventive Medicine, Graduate School of Medicine, The Univ. of Tokyo, 7-3-1 Hongo, Bunkyo-ku, Tokyo 113-0033, Japan*

(Received February 17, 2009)

**ABSTRACT** — We have recently reported breakdown of mucosal immunity in the gut by tetraclorodibenzo-p-dioxin (TCDD). That is, single oral administration of low dose 2,3,7,8-TCDD resulted in a marked decrease in IgA secretion in AhR-dependent manner and impaired oral tolerance in the gut. In the present study, we found TCDD exposure by breast feeding also resulted in decreased level of IgA in the gut. Ig production by B cells by LPS stimulation was not affected by TCDD administration. Instead, particular chemokine receptor expression on B1 cells, a major cell source for intestinal IgA antibody, was decreased in mice treated with TCDD. In consistence with this observation, B1, but not B2 cells from TCDD treated mice showed impaired chemotaxis towards B lymphocyte chemokine (BLC)/CXCL13. In contrast, chemotaxis of intestinal dendritic cells (DCs) towards secondary lymphoid-tissue chemokine (SLC)/CXCL19 was not impaired in mice treated with TCDD. Furthermore, there was no change in the number and profile of intesitinal microflora in TCDD-treated mice. These results indicate that TCDD exposure by breast feeding results in breakdown of intestinal mucosal immunity of pups and that it may be attributed in part to impaired B1 cell migration from the peritoneal cavity to intestinal mucosa.

**Key words:** TCDD, Mucosal immunity, IgA, Oral tolerance, Allergy

## INTRODUCTION

2,3,7,8-tetraclorodibenzo-p-dioxin (TCDD) has been reported to exert a variety of adverse effects on immune responses including antibody production and cytotoxic T lymphocyte (CTL) generation (Hollsopple *et al.*, 1991; Kerkvliet, 1995, 2002). Exposure to TCDD also results in decreased resistance to several infectious agents (Warren *et al.*, 2000). However, immunological effects of dioxins on mucosal immunity in the gut have not been intensively examined so far despite that most dioxins are exposed through the digestive tract. Intestinal mucosal immunity is characterized by massive IgA secretion into the gut lumen and induction of oral tolerance against huge amounts and kinds of dietary antigens. Both intestinal IgA and oral tolerance play pivotal roles for body defense to protect against pathogens and to avoid systemic allergic sensitization by oral antigens (Strobel and Mowat, 1998; Faria and Weiner, 1999). We previously demonstrated that mucosal immunity in the gut was impaired in BWF1 mouse strain, a murine model for systemic lupus erythematosus (SLE) (Akadegawa *et al.*, 2005). Aged BWF1 mice developing lupus nephritis showed a defective IgA secretion in the gut and increased susceptibility to bacterial infection. Oral tolerance was also impaired and orally administered-antigens induced systemic allergic sensitization in the respiratory tract in these mice. On the other hand, it is well recognized that allergic diseases have been increasing for the recent several decades in developed countries and that environmental factors are more involved in disease increase than genetic factors (Schultz-Larsen, 1993). These environmental factors include increased air pollution, dust mite, dietary antigens, environmental chemicals and so on (Hopkin, 1997). We hypothesized that environmental chemicals which disrupt mucosal immunity in the gut would result in allergic sensitization by oral antigens

Correspondence: Sho Ishikawa (E-mail: yamasho@m.u-tokyo.ac.jp)

and could be a critical environmental factor for increased allergic diseases. In fact, we found that administration of low-dose TCDD resulted in defective IgA secretion in the gut in an AhR-dependent manner and in breakdown of oral tolerance leading to antigen-specific systemic sensitization (Kinoshita *et al.*, 2006).

In the present study, we suggest that TCDD exposure by breast feeding also results in decreased level of IgA in the gut of pups and that impaired chemotaxis of a particular B cell subset may be one of the possible mechanisms for TCDD-induced breakdown of mucosal immunity in the gut.

## MATERIALS AND METHODS

### Mice

Specific pathogen-free C57BL/6 mice, originally obtained from the Shizuoka Laboratory Animal Center (Shizuoka, Japan), were maintained under SPF condition in our animal facility at The University of Tokyo. 2,3,7,8-TCDD (Daiichikagaku Co., Tokyo, Japan) in corn oil was intragastrally administrated to mothers 3 days after delivery and fecal IgA level of pups was measured every 2 weeks. In some experiments, adult C57BL/6 mice aged 6-8 weeks were used. All animal experiments complied with the standards set out in the guidelines of the University of Tokyo.

### Cell preparation

Peritoneal B1 cells were purified by MACS® magnetic beads (Miltenyi Biotech, Bergisch Gladbach, Germany) from whole peritoneal cells. Briefly, T-cells, macrophages and B2 cells were depleted by incubating with a biotinylated mAb cocktail (anti-Thy1.2, anti-F4/80 plus anti-CD23 mAbs) followed by incubation with streptavidin-conjugated magnetic beads. Splenic B2 cells and $CD4^+$ T cells were also isolated by MACS beads conjugated with anti-mouse B220 or anti-mouse CD4 mAb. Cell purity was more than 90% throughout the experiments.

### ELISA for fecal IgA

One-hundred milligrams of fecal pellets were placed into 1.5 ml microcentrifuge tubes, added 1 ml (10 volumes, w/v) of phosphate buffered saline (PBS), and incubated at room temperature for 15 min. Samples were vortexed, left to settle for 15 min, revortexed until all material was suspended, then centrifuged at 12,000 rpm for 10 min. The supernatant was removed and stored at −80°C or immediately tested on ELISA kit for IgA (Bethyl Laboratories, Montgomery, TX, USA). Microtiter plates were coated with goat anti-mouse IgA affinity purified antibody and incubated for 60 min. Plates were washed with PBST (PBS containing 0.05% Tween 20) and each well was blocked with 200 µl of 50 mM Tris (pH 8.0) containing 0.15 M NaCl and 1% bovine serum albumin (BSA) for 30 min. After washing with PBST, 100 µl of test samples and standards was added per well and incubated for 60 min. Horse radish peroxidase (HRP) labeled goat anti mouse IgA-Fc specific Ab was added to each well and incubated for 60 min. Color was developed with HRP substrate (3,3',5,5'-tetramethyl benzidine) for 30 min and read at 450 nm with a Emax® precision microplate reader (Molecular Devices Corporation, Sunnyvale, CA, USA).

### Flow cytometry

FITC-conjugated anti-CD4 (GK1.5), anti-CD5 (53-7.3RRH) and anti-CD11b (M1/70); PE-conjugated anti-CD8α (53-6.7), anti-CD11c (HL-3), anti-B220 (RA3-6B2); and APC-conjugated anti-B220 (RA3-6B2) mAbs were purchased from PharMingen (San Diego, CA, USA). Lymphoid cells were stained with 1) FITC-conjugated anti-CD4, PE-conjugated anti-CD8 and APC-conjugated anti-B220 mAbs, or 2) FITC-conjugated anti-CD5 and PE-conjugated anti-B220 mAbs, or 3) FITC-conjugated anti-CD11b and PE-conjugated anti-CD11c mAbs and analyzed on Epics Elite® cell sorter (Coulter Electronics, Hialeah, FL, USA).

### Induction of oral tolerance

Induction of systemic unresponsiveness to OVA (Sigma Chemical Co., St. Louis, MO, USA) was performed as described previously [7]. Briefly, mice were given 25 mg of OVA in 250 µl PBS by gastric intubation at day 0. Control mice received PBS. At day 7 and 21, mice were immunized and challenged subcutaneously (s.c.) with 100 µg OVA in 100 µl CFA (Difco Laboratories, Detroit, MI, USA). OVA-specific Ab in the serum was measured 7 days after the second s.c. immunization.

### OVA induced cell proliferation assay

Twenty-five mg of OVA in 250 µl PBS was administrated intragastrally three times in a week after TCDD treatment (day 0). Two weeks after the last administration, spleen and lymph nodes (axillar, pulmonary, mesenteric, renal, inguinal) were removed aseptically. Single-cell suspensions were obtained using fine-mesh screens (Cell Strainer, Becton Dickinson, Franklin Lakes, NJ, USA). $4 \times 10^5$ cells were cultured in the presence of OVA or KLH (200 µg/ml) for 5 days at 37°C in 5% $CO_2$ in atmosphere. Each well was pulsed with $^3$H-thymidine (1 µCi/ml) for the last 18 hr of the culture. Cells were then harvested

onto a glass filter and radioactivity was counted with a liquid scintillation counter.

### Chemotaxis assay

Chemotaxis assay using ChemoTx plate (Neuro Probe, Gaithersburg, MD, USA) was performed according to manufacturer's instructions. Briefly, spleen cells were suspended at $10^6$ cells/ml in RPMI 1640 medium containing 0.5% BSA and 20 mM HEPES. Sixty μl of cell suspension was loaded on the membrane plate and placed onto a flat-bottomed microtiter plate with 96 wells containing 30 μl of serially-diluted B lymphocyte chemokine (BLC) solution in each well. The plate was then incubated at 37°C for 90 min and migrated cells were collected. Cells were then stained with FITC-labeled anti-CD5 and PE-labeled anti-B220 mAbs and counted on EPICS ELITE cell sorter. Chemotaxis assays for B1 and B2 cells were performed on the same plate and on the same day in each experiment because the absolute migrated cells varied in each chemotaxis assay. For chemotaxis assay for purified B1 and B2 cells, the mixture of 5 x $10^6$ spleen and the peritoneal cells from young BWF1 mice was stained with FITC-labeled anti-CD5 and PE-labeled anti-B220 mAbs and subjected to cell sorting using EPICS ELITE cell sorter. The purity of B1 and B2 cells was more than 95% in all experiments.

### DNA chip analysis

Total cellular RNA was prepared from B1 cell obtained TCDD-treated mice and DNA chip analysis performed using A24 GeneChips (Affmetrix, Santa Clara, CA, USA). Gene expression was confirmed by real-time PCR using ABI PRISM 7500 (Applied Biosystems, Foster City, CA, USA).

### Statistical analysis

Statistical analysis was performed using Student's t-test. The 95% confidence limit was taken as significant.

## RESULTS

### Decreased IgA secretion in the gut by oral administration of TCDD

To investigate immunological effects of TCDD on intestinal mucosa, C57BL/6 mice were intragastrally administered various doses of TCDD and fecal IgA level determined by ELISA. The level of fecal IgA was dose-dependently decreased in mice treated with TCDD (Fig. 1, Modified from EHPM 11:256-263, 2006). It should be noted that relatively low doses of TCDD (0.1 μg/kg and

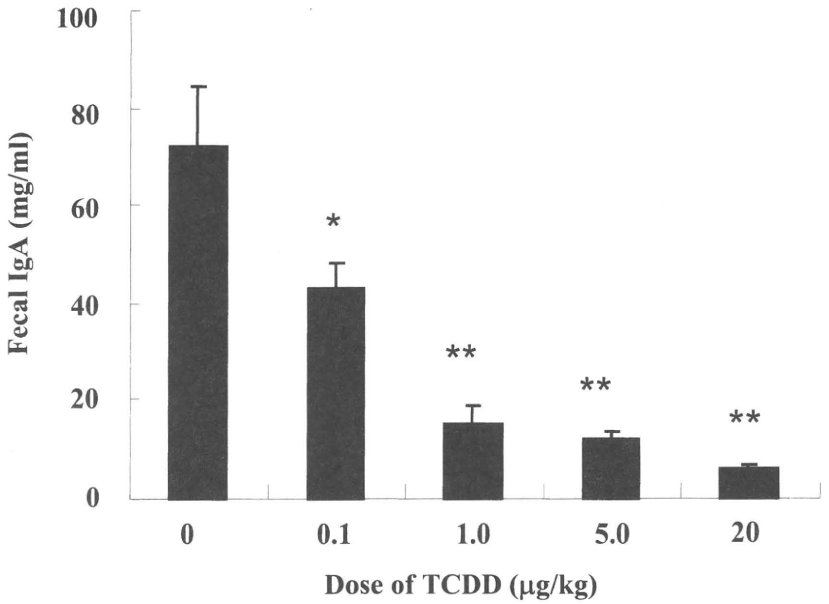


Modified from Env. Health. Prev. Med. 11:256-263, 2006

**Fig. 1.** TCDD suppresses IgA secretion in the gut. Dose-ependent IgA suppression by TCDD. C57BL/6 mice (n = 5) were intragastrally administered with TCDD (0.1, 1.0, 5, 20 μg/kg) and fecal IgA level was determined by ELISA 1 week after TCDD treatment. Monoclonal IgA Ab was used as control. The mean concentration ± S.D. were presented in each graph. A representative result from four independent experiments is presented.

1.0 μg/kg) significantly inhibit IgA secretion into the gut lumen. IgA level returned to the normal level by 4 weeks after administration of 1 μg/kg TCDD (data not shown). To examine whether or not the inhibitory effect of TCDD on IgA secretion in the gut is mediated by AhR, a specific receptor for TCDD, fecal IgA level in AhR-deficient mice administered TCDD (1 μg/kg) was examined. The inhibitory effect of TCDD on IgA secretion in the gut was totally abrogated in AhR-deficient mice with C57BL/6 background while heterozygous littermates and C57BL/6 mice showed a marked decrease in IgA secretion in the gut (Fig. 2, Modified from EHPM 11:256-263, 2006). To examine the effect of TCDD exposure through breast feeding, mother mice were orally administered TCDD 3 days after delivery and fecal IgA level of pups measured by ELISA. As shown in Fig. 3 (Modified from EHPM 11:256-263, 2006), fecal IgA level was decreased in pups exposed to TCDD through breast feeding. It should be noted that the effect of TCDD on fecal IgA levels was more prominent in male than female mice.

### Effect of TCDD on oral tolerance

Oral tolerance is historically and originally described as antigen-specific inhibition of antibody production by oral pre-administration of protein antigen. As shown in Fig. 4 (Modified from EHPM 11:256-263, 2006), OVA-specific IgG production was suppressed in mice which had been orally administered OVA before systemic immunization, demonstrating that oral tolerance was induced in these control mice. Oral administration of KLH did not inhibit OVA-specific IgG production (data not shown). In contrast, the suppression of IgG production was partially abrogated in TCDD treated-mice, suggesting a breakdown of oral tolerance. In consistence with the impaired oral tolerance in TCDD treated-mice, T-cells in PPs, axillar, inguinal, cervical LNs, and spleen of TCDD-treated mice were antigen-specifically sensitized and proliferated in the presence of OVA *in vitro* while KLH stimulation

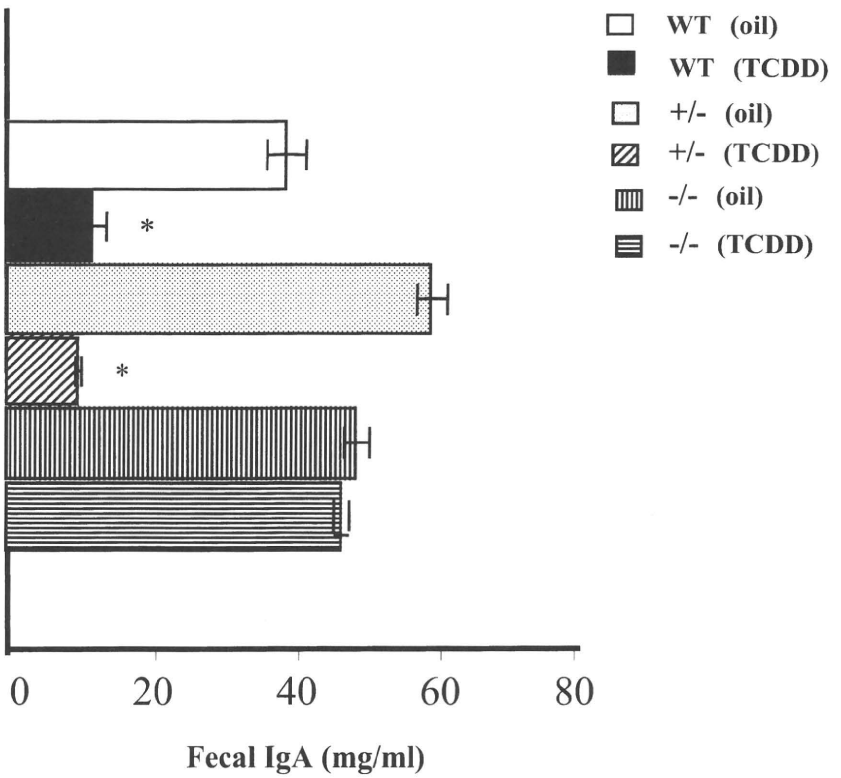


Modified from Env. Health. Prev. Med. 11:256-263, 2006

**Fig. 2.** AhR dependent suppression of IgA secretion in TCDD-treated mice. TCDD (1 μg/kg) or corn oil was given to C57BL/6 (WT), AhR heterozygous (+/-), AhR deficient (-/-) mice and fecal IgA level was determined by ELSA 1 week after TCDD treatment (n = 5). A representative result from two independent experiments is presented. Statistical analysis was performed by Student's *t*-test. * $p < 0.001$.

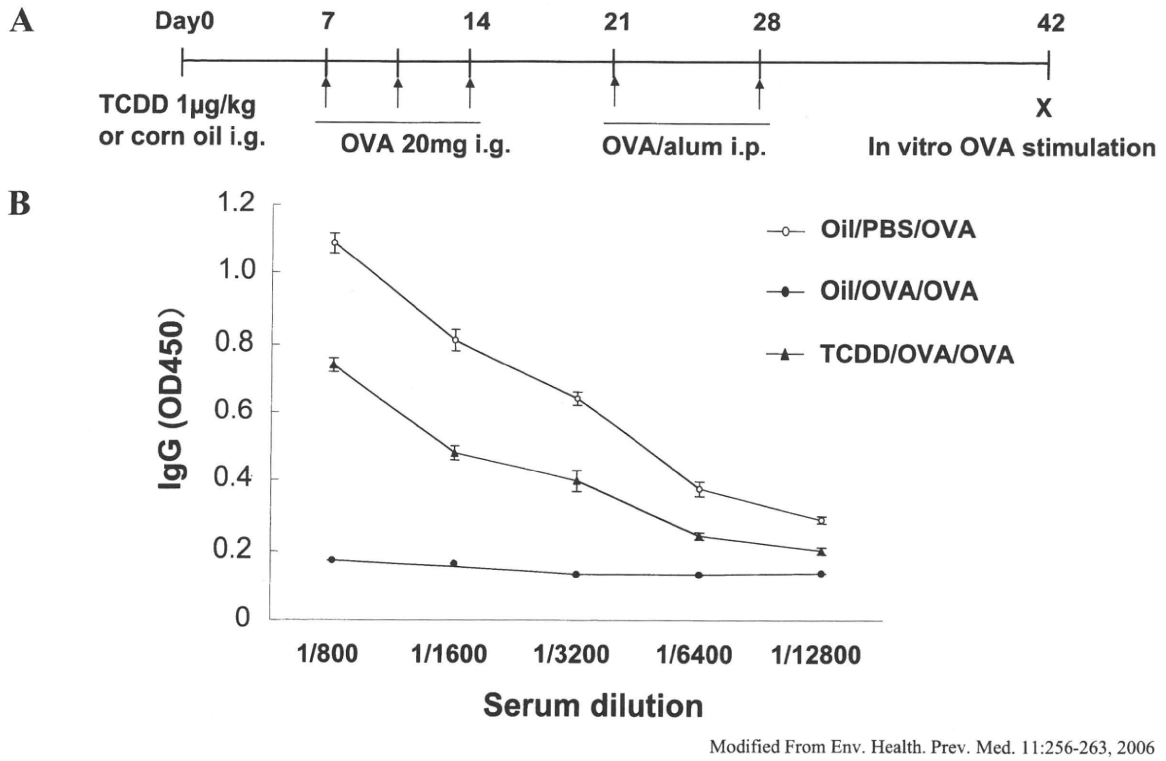


Modified From Env. Health. Prev. Med. 11:256-263, 2006

**Fig. 3.** Breakdown of oral tolerance and systemic sensitization by oral antigens and intact antigen uptake in TCDD-reated mice. Mice were treated with TCDD (filled square, ■) or corn oil (open triangle, Δ) at day 0 and orally administered 25 mg of OVA at day 7 and 14. Then mice were immunized s.c. with 100 μg of OVA in CFA at day 21 and day 28 (n = 4). Mice immunized with OVA plus CFA were used as positive control (open diamond, ◊). The serum concentration of OVA specific IgG antibody at day 35 was determined by ELISA. The results are expressed as the mean ± S.D.. A representative data from three experiments is presented. * $p < 0.001$.

did not induce cell proliferation (Fig. 5).

### Mechanisms for decreased IgA levels in TCDD-treated mice

There was no histological change in the intestine of TCDD-treated mice and Alexa-488 labeled OVA was incorporated into the subepithelial dome of PPs normally (data not shown). Fluorescent activated cell sorter (FACS) analysis also showed no significant change in the frequency of cellular subset of immunocompetent cells in lymphoid tissues including mesenteric LNs and PPs (data not shown). In particular, frequency of $IgA^+$ B-cells in the Peyer's patches and mesenteric LNs remained unchanged in TCDD-treated mice (Fig. 6A, Modified from EHPM 11:256-263, 2006). Furthermore, serum IgA level was not decreased in TCDD-treated mice (Fig. 6B, Modified from EHPM 11:256-263, 2006). Decreased level of IgA in the gut was not attributed to direct effect of TCDD on Ig production because *in vitro* IgM secretion by B-cells by LPS stimulation was not affected by TCDD treatment (Fig. 7). DNA chip analysis revealed that 231 genes were increased and 1,096 genes decreased in B1-cells obtained from TCDD-treated mice (Fig. 8). Real time PCR analysis confirmed that expression levels of particular chemokine receptors such as CCR2, CCR7, CXCR4 and CXCR5 were decreased in B1-cells obtained from TCDD-treated mice (Fig. 9). In consistence with this observation, chemotactic activity of B1, but not B2 cells towards BLC/CXCL13 was impaired in TCDD-treated mice (Fig. 10). On the other hand, $CD11c^+$ cells obtained from PPs and mesenteric LNs of TCDD-treated mice did not show impaired chemotaxis towards secondary lymphoid-tissue chemokine (SLC)/CCL21 (Fig. 11). Furthermore, the number and frequency of major commensal bacterial species which were believed to play a role in the maintenance of oral tolerance were not changed in TCDD-treated mice (Fig. 12).

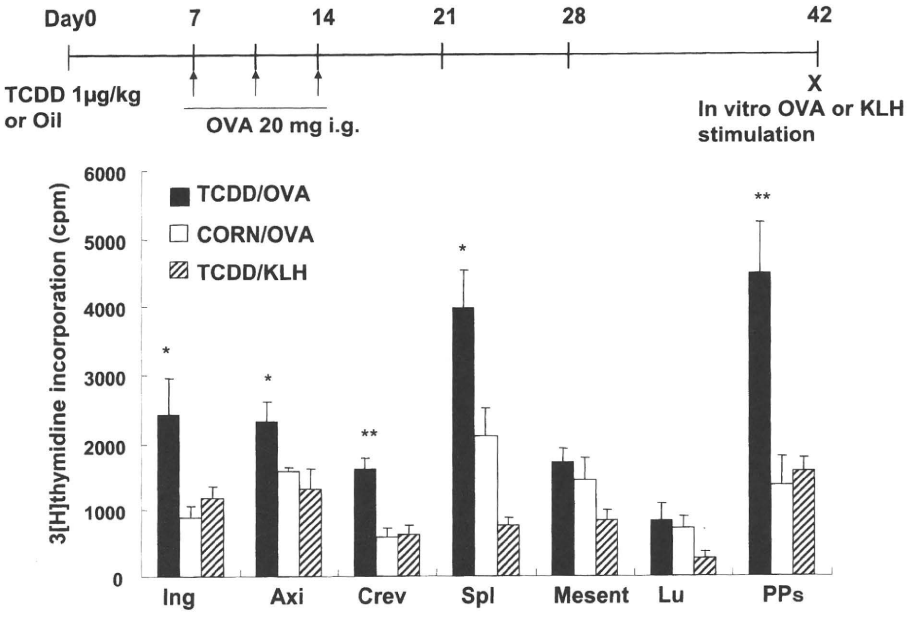


Modified From Env. Health. Prev. Med. 11:256-263, 2006

**Fig. 4.** Systemic sensitization with orally administered OVA by TCDD pretreatment. Mice were treated with TCDD on day 0 and then mice were intragastrally given 25 mg of OVA twice at day 7, 10 and 14. At day 28, single cell suspensions were obtained from spleen (Spl), inguinal (Ing), axillar (Axil), mesenteric (Mes), pulmonary (Pulm) lymph nodes, and Peyer's patches (PPs) and stimulated *in vitro* with OVA or KLH (200 μg/ml) at 37°C for 5 days. Cell proliferation was measured by $^{3}$H-thymidine incorporation as described in Material and Methods. Results are presented as the means ± S.D. (n = 4). A representative data from three experiments is presented. *p < 0.05, **p < 0.01.

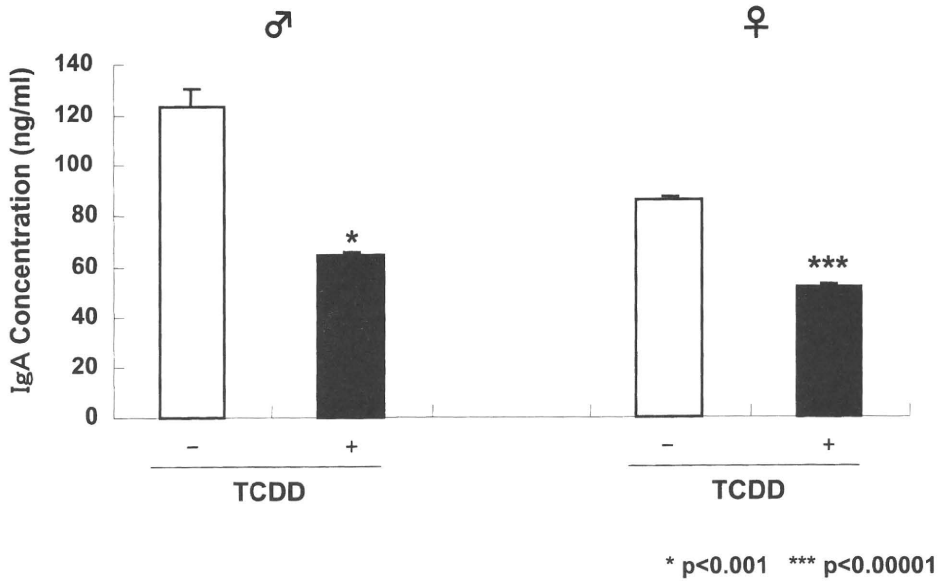


**Fig. 5.** Effect of TCDD exposure through mother milk on fecal IgA level of pups. TCDD was administered to mother 3 days after birth and fecal IgA levels of pups measured by ELISA 4 weeks after delivery (n = 5 or 6).

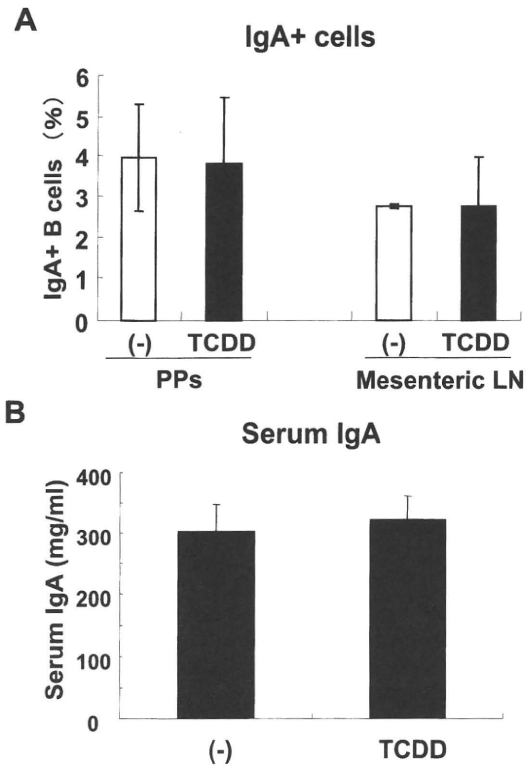


Modified From Env. Health. Prev. Med. 11:256-263, 2006

**Fig. 6.** No change in the frequency of $IgA^+$ cells and serum level of IgA in TCDD-treated mice. **A.** Cells prepared from PPs or mesenteric LNs were stained with FITC-anti-IgA, PE-anti-B220, and APC-anti-CD19 Abs. The percentages of $IgA^+B220^+$ cells in $CD19^+$ cells were presented (n = 3). **B.** Serum concentration of IgA in TCDD-treated and control mice (n = 3) was measured by ELISA as described in Materials and Methods.

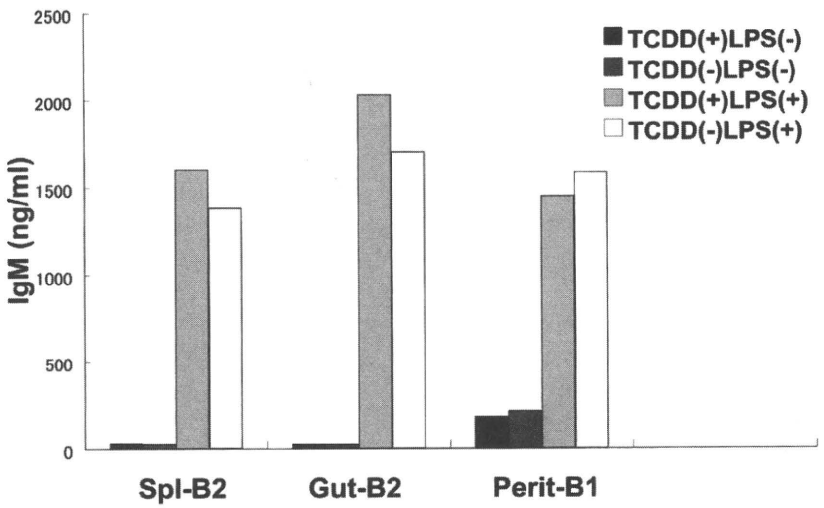


**Fig. 7.** Unimpaired IgM production by B1 and B2 cells on stimulation with LPS. B1 and B2 cells from TCDD-treated or control mice were stimulated *in vitro* in the presence of LPS (5 mg/ml) and IgM concentration in the culture supernatant was measured 5 days after stimulation.

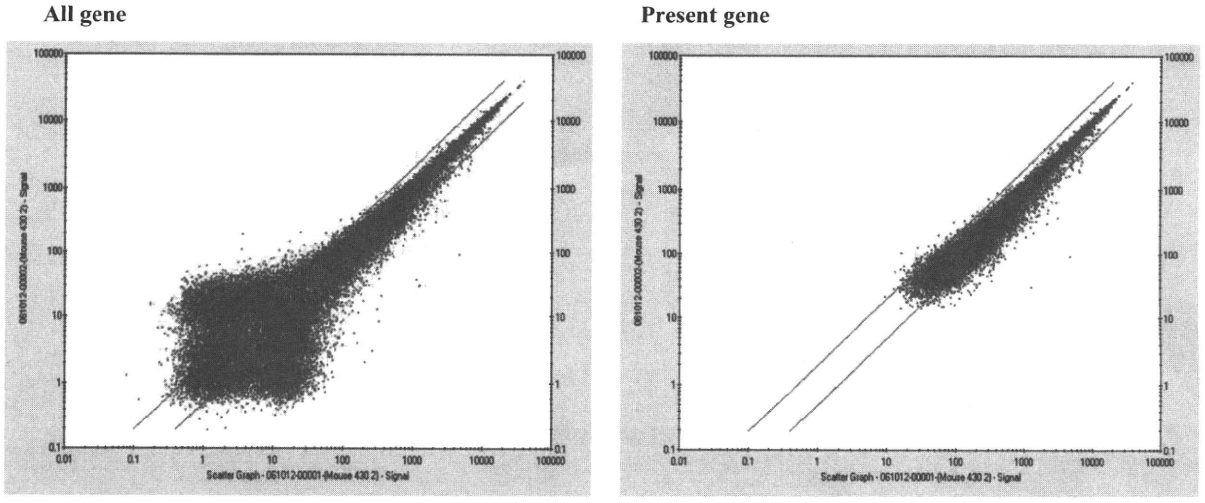


**Fig. 8.** DNA chip analysis on TCDD-treated B1 cells. Total cellular RNA was prepared from B1 cells obtained from TCDD-treated mice 1 week after injection and subjected to DNA chip analysis as described in Materials and Methods. Significant expression levelsof genes are dotted as present genes.

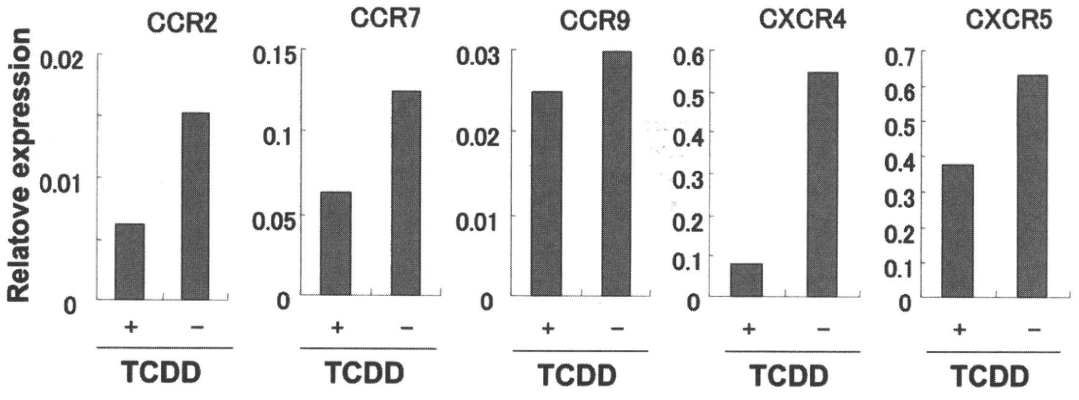


**Fig. 9.** Decreased expression of chemokine receptors in B1-cells in TCDD-treated mice. Total cellular RNA was prepared from sorted B1 cells from TCDD-treated or control mice and expression levels of chemokine receptors were measured by real-time PCR.

## DISCUSSION

We previously reported breakdown of mucosal immunity in the gut by a single oral administration of 2,3,7,8-TCDD (Kinoshita *et al.*, 2006). That is, relatively low-dose TCDD administration resulted in a marked decrease in IgA level in the gut in an AhR-dependent manner and impaired oral tolerance in the gut. The mechanism for decreased IgA level in the gut, however, remained to be elucidated. There was no histological change in the intestine in TCDD-treated mice. Cellular subsets of immunocompetent cells in lymphoid tissues including PPs, spleen, thymus and peripheral LNs also remained unchanged. The frequency of $IgA^+$ B-cells was not decreased in the mesenteric LNs and PPs in TCDD-treated mice in FACS analysis whereas those in the intestinal lamina propria were decreased in immunofluorescent study in TCDD-treated mice. In the present study, we found that expression levels of par-